NASA CONTRACTOR
REPORT

NASA CR-1138

NASA CR-11

AN ANNULAR LITHIUM-DRIFTED GERMANIUM DETECTOR FOR STUDYING NUCLEAR REACTION GAMMA-RAYS

by A. J. Levy, R. C. Ritter, and K. Ziock

Prepared by
UNIVERSITY OF VIRGINIA
Charlottesville, Va.
for

NATIONAL AERONAUTICS AND SPACE ADMINISTRATION • WASHINGTON, D. C. • SEPTEMBER 1968

NASA CR-1130

AN ANNULAR LITHIUM-DRIFTED GERMANIUM DETECTOR

FOR STUDYING NUCLEAR REACTION GAMMA-RAYS

By A. J. Levy, R. C. Ritter, and K. Ziock

AN ANNULAR LITHIUM-DRIFTED GERMANIUM DETECTOR

FOR STUDYING NUCLEAR REACTION GAMMA-RAYS

By A. J. Levy, R. C Ritter and K. Ziock

Department of Physics
University of Virginia

Abstract

A fabrication technique has been developed for truly annular Ge(Li) gamma detectors. Featuring spark-cutting to precisely control the un-damaged germanium volume, the detector is capable of standard-geometry techniques such as are used with NaI detectors.

In this report, background material relevant to the annular geometry is presented. An extremely explicit, detailed description of the complete fabrication procedure is given, including special cutting, radiant diffusion, and drifting techniques developed here.

Measured properties of several detectors are presented, with the emphasis being on the usefulness of the detector for high energy gamma ray spectra.

AN ANNULAR LITHIUM-DRIFTED GERMANIUM DETECTOR

FOR STUDYING NUCLEAR REACTION GAMMA-RAYS

The Lithium-Drifted Germanium detector represents the most advanced
stage in a systematic development of semiconductor materials and devices made
from them for the purpose of radiation detection. The semiconductor detector
described herein has a distinct similarity to the gaseous ionization chamber,
but its superiority for most applications is notable.

The higher density of the semiconductor material makes complete absorp-
tion of most charged particles certain. The higher atomic number, especially
of germanium, coupled with several other advantages discussed below, makes the
solid-state analogue of the ionization chamber extremely attractive as a
detector of gamma-rays. But in the energy region where germanium detectors
are most useful because of the excellent energy resolution, i.e., 0.3 to 10
MeV, they are, at present, very inefficient, especially when compared to the
large NaI scintillation crystal. This report presents the results of a pro-
gram to produce detectors with greatly improved efficiency, while maintaining
the features which have proved to be so desirable in a gamma detector.

Background material will be presented as it applies to the specific re-
search problems. There are several rather complete general reviews of semi-
conductor radiation detectors in print[1-5].

A. Fundamental Considerations

1. Charge Production

The conversion of the photon energy to a usable electrical signal
is achieved by the transfer of energy to an electron, either by the photo-
electric or Compton effects, or by the production of an electron-positron pair.
It is primarily the number of electrons produced and collected at the contacts

that gives the germanium lithium-drifted detector (abbreviated herein according to present convention as Ge(Li)) its excellent energy resolution. The energy required to produce one electron-hole pair in germanium is $\epsilon = 2.9$ eV at 77°K compared with an average value of 30 eV for most gases and 3.6 eV for silicon. This means that, if straightforward Poisson statistics are used, the statistical fluctuations of the signal will be approximately 1/3 as much in germanium as in gaseous devices. In practice, a much greater improvement is observed.

Fano, from consideration of ionization in gases[6] predicts that the fluctuation in the number of pairs will be less than that predicted by Poisson statistics. The yield of charge carriers is given by

$$N = E/\epsilon$$

If a variance, N', is observed in the signal produced[*], then (excluding effects of electronics noise) the Fano factor is defined as the ratio of the variance to the yield.

$$F = N'/N$$

If F were equal to unity, then the energy loss mechanism that produces an electron-hole pair would be independent of all other pairs produced. Because the pairs are formed in the last stages of a branching process in the semiconductor material, the last of the secondary electrons have only a few times the energy necessary to produce a pair. There is a stringent boundary condition to meet, since the energy needed to form a pair is an invariant quantity and only integral numbers of pairs can exist. It is this boundary condition, primarily, that leads to non-random production of pairs in the semiconductor and the ensuing departure from Poisson statistics. Van Roosbroeck[7] predicts,

---

[*]The full width at half maximum of the observed peak is 2.35 times the square root of the variance.

from a mathematical model of the branching process, a Fano factor of 0.32. It is now believed that this number is too high and Fano factors have been measured from 0.30[8] to as low as 0.16[9]. Mann[10] has reported a Fano factor of $0.055 \pm .003$ for one detector.

As the number of electron-hole pairs produced is proportional to the energy of the incoming particle, regardless of particle type, the response of semiconductor detectors is linear with energy. The integral linearity has been shown to be better than 0.2% from 0.2 to 8 MeV[11]. This linearity depends on complete collection of the charge produced.

2. Charge Collection

In order to take advantage of the large amount of charge released by a charged particle or secondary electron from a photon interaction, proper charge collection must be realized. The most straightforward method to achieve this is to apply a sufficient electric field to attract the free charge liberated by ionizing radiation to the collecting electrode. This method, which uses a block of intrinsic semiconductor material referred to as a homogeneous bulk counter, was the method first tried. It was partially successful with silicon, but suffered the malady that the "dark current", i.e., the current present due to thermally generated carriers, dominated that from the radiation. Even with the purest silicon available the difficulties were forbidding. With germanium the situation is much worse as the probability of generating charge carriers due to thermal energy is much greater. Cooling germanium to $77^{\circ}K$ does not eliminate the difficulty.

The n-p diode junction has the property that between the two doped regions, one rich in doners (electrons) and the other rich in acceptors (holes), there is a region which is depleted of carriers. With the diode junction reversed biased, the width of the depleted region is a function of the applied

4

bias voltage. It increases as the square root of the voltage in the simple junction counter.

If the crystal, germanium in this case, is cooled to 77°K the free carrier density arising from thermal generation is negligible. In this situation the applied field is concentrated within the depleted region and in the case of planar geometry the field is uniform. The effective volume of the detector is therefore only the volume of the depletion region. One of the most fundamental difficulties in achieving the optimum energy resolution, arises in the process of collecting the charged produced. There are several causes of incomplete charge collection, but for the case of gamma-produced secondary electrons, there is one which far exceeds all others in importance. With gammas incident on the crystal, the charge is created throughout the detector volume and the electron or hole may have to traverse all possible values of the depletion width, d. This alone would not cause serious difficulty if it were not for the presence of trapping or recombination centers. These centers are the most important impedance to complete charge collection. All samples of germanium have these centers, and they result from either impurities, or crystal imperfections. They may either scatter a carrier or detain it, thus increasing the probability for recombination with a carrier of opposite type. If we assign to the electrons a most probable traversal before being trapped, called the drift length, l_n and to the holes a drift length, l_p, we can then examine the effect of trapping on the energy resolution of the detector[12].

The calculations for this effect have been carried out by Northrop and Simpson[13] with the following results: The average charge collected, whether the sum of the drift lengths for electrons and holes is greater or less than the depletion width is,

$$\bar{g} = \frac{(\ell_n + \ell_p)}{d} - \frac{(\ell_n^2 + \ell_p^2)}{2d^2} \quad Ne \quad,$$

and the variance in the signal is given by

$$\sigma^2 = \frac{(\alpha^3 + \beta^3)}{3} - \frac{(\alpha^2 + \beta^2)}{4} \quad N^2 e^2 \quad,$$

where for the case $\ell_n + \ell_p < d$

$$\alpha = \frac{\ell_n}{d} \quad \text{and} \quad \beta = \frac{\ell_p}{d}$$

and for the case $\ell_n + \ell_p > d$

$$\alpha = 1 - \frac{\ell_n}{d} \quad \text{and} \quad \beta = 1 - \frac{\ell_p}{d} \quad .$$

In the second case, the electrons and holes are both collected. It is now possible to plot the resolution of the detector as a function of the electron and hole drift length and the size of the detector. This has been done and is shown in Figure 1. The relative RMS spread is plotted in three dimensions. It is observed that the function has zeroes at $l_p = l_n = 0$ and $l_p = l_n = d$. The former zero corresponds to zero charge collected and is hardly meaningful. The latter corresponds to complete charge collection regardless of the entry point of the incident radiation, as might have been expected.

The area of most interest is where the two relative drift lengths are equal to 0.4. It can be seen from Figure 2, (the cross section of the resolution function at $l_n = l_p$), that for values of $l_p = l_n$ less than this value, an increase in the field strength, which will of course increase l_p and l_n, the resolution becomes worse even though the total charge collected increases. Also it is clear that for any value of l_p, the smallest energy spread occurs when $l_n = l_p$. As the linear dimensions of the detector become greater, it becomes necessary to increase the field strength so that the drift length is
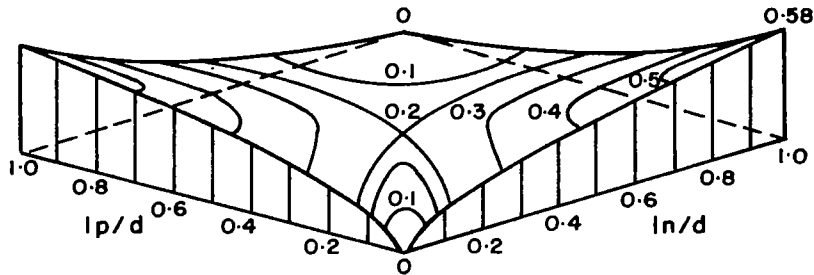
Figure 1. Resolution of a semiconductor detector
vs. charge collection efficiency. After
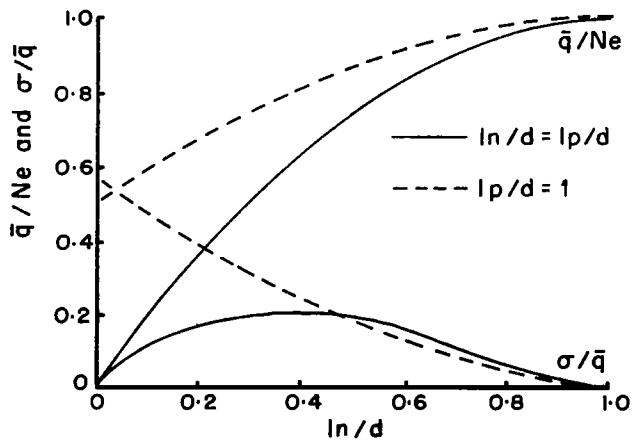Northrop and Simpson[12].

Figure 2. Charge collection efficiency and
resolution vs. electron collection efficiency.
After Northrop and Simpson[12].

a maximum value consistent with the conditions for minimum resolution. This can only be done as long as the electrons remain in thermal equilibrium with the crystal lattice[12]. It is this criterion that will ultimately limit the size that can be attained.

According to Shockley[14], the maximum drift velocity that can be attained before thermal noise begins to increase appreciably is the velocity of sound in the crystal. Also it is worthy to note that the drift velocity decreases when the field strength is made too high. Since this value is above 1000V/cm in germanium, there are more important effects that limit the applied field. This will be discussed as a part of the operating procedure of the lithium-drift detector.

A variation of resolution with the drift length of the charge carriers arises from the fact that the drift mobilities of the holes and electrons have different dependences on the crystal temperature. Variation with the actual impurity concentration in the particular germanium sample used is also observed. This leads to a variation with temperature of the resolution besides the expected effects of the reduction of thermal energy (which always is monotonic decreasing with a reduction of crystal temperature). Since the optimum resolution occurs when the hole and electron drift lengths are equal, it is to be expected that there will be several local minima in the resolution as the temperature is decreased, and an absolute minimum when the thermal energy is well below that needed to excite an electron into the conduction band. As temperature is further lowered, the resolution will change as is dictated by the relative variation of l_n and l_p.

Tavendale has shown[5] that the resolution changes very little below 160°K, but there is a broad minimum in resolution occurring in the region of 70° to 80°K. This indicates that in this region for crystalline field the hole and

electron drift lengths are equal; a fortuitous situation indeed, since this is a singularly easy temperature to maintain. For one sample of germanium an absolute minimum has been observed several degrees above liquid nitrogen temperature*.

However the situation has only been studied in detail for crystalline electric fields. It is the purpose of this part of the report to describe a germanium detector in which the field is radial (cylindrical). Since the electrons are always traversing a decreasing field, and the holes always traverse an increasing field, it is not sufficient to assume that the same conditions for minimum resolution will prevail for a radial field. Due to the extreme difficulty of controlling temperatures accurately in the region of $50°$ to $100°K$, this study has not been undertaken as part of the current work being reported here, but is worthy of consideration in future research. As will be shown later, the principal cylindrical detector used in the measurements described in the second part of the report was operated under conditions for which the charge collection was invariant with field strength, indicating that the drift length of both holes and electrons was greater than the radial width of the depletion region.

B. The Lithium-Drift Principle

The diode junction counter mentioned above is nearly useless for the detection of gamma-rays, since the depth that can be produced by maximizing the bias voltage, in the best material available, is of the order of 1 millimeter. (Beyond a certain electric·field strength the conduction electron can no longer transfer the accumulated energy between collisions. Shockley[12,15] calls these carriers "hot electrons" and shows that the noise increases very rapidly with electric field at this point.)

---

*I. Fowler, Private Communication, March 3, 1966.

It is therefore necessary to increase the active depth of the counter by other means than high fields.

Whereas the homogeneous counter attempts to provide a totally intrinsic or "i" region for detection, it fails in the respect that donors can not be eliminated from the material that injects electrons into the conduction band, and acceptors are ever-present, detaining electrons and increasing the probability of recombination. The equivalent effects regarding holes presented equal difficulties. A result of these effects is the unavoidable generation of excessive noise currents. The Ge(Li) represents a hybridization of the homogeneous type "i" counter, with the n-p junction counter.

The n-i-p structure is most nearly an analogue of the ionization chamber, with the n and p layers serving as the electrode contacts[16-18].

For the detector to exhibit optimum characteristics, the intrinsic region must be as free of donor or acceptor sites as possible. This is not accomplished by refining the basic material to reduce the impurities, and a method to render these sites ineffective as acceptors or donors must be employed. If material is used that has an excess of acceptors (called "p" type) it becomes efficient to use a method of compensating these impurity sites by a method called lithium drifting[19]. At room temperature lithium is relatively mobile in germanium and is able to form an ion pair with the acceptor impurity. This ion pair has a much smaller electric field than either the acceptor site or the lithium ion alone, hence the acceptor site is effectively removed as a scatterer of carriers by its electric field. Furthermore, the lithium donor and acceptor are, in effect, removed from the band gap and their contribution to trapping and recombination is markedly reduced. When the detector is cooled to operating temperature, around $77^{\circ}K$, the lithium becomes immobile (for all practical purposes) thereby creating a stable region whose apparent properties

are very nearly those of intrinsic material with a negligible concentration of acceptors.

1. Introduction of the Lithium to the Germanium

The lithium is usually introduced into the germanium in the form of a supersaturated solution by first coating the surface of the germanium and then diffusing the lithium at a high temperature for a short time. The initial lithium distribution produced in this way is described by[*]

$$N_D = N_0 \ \text{erf} \left[\frac{x}{2\sqrt{Dt}} \right] \quad ,$$

where N_D is the donor concentration at a distance, x, from the surface and N_0 is the donor concentration at the surface. D and t are the diffusion constant and diffusion time respectively. The initial acceptor concentration is uniform and can be calculated by the expression

$$N_A = \frac{1}{qR\mu_p} \quad ,$$

with q = 4.8 x 10^{-10} esu, R = 9.5 ohm-cm, and μ = 1800 cm^2-V-sec, N_a = 3.7 x 10^{14} per cm^3. The distribution for this case is plotted in Figure 3. The resultant carrier concentration in the region of .58 mm is very nearly zero, being populated by equal amounts of donors and acceptors. To the left, i.e., towards the surface, the donor concentration due to the lithium rises very quickly and because of this the sheet resistance of the diffused surface is very low.

At depths greater than 0.58 mm, the concentration is largely due to the initial acceptor density, being relatively unaffected by the diffusion. The crossover point is of considerable interest. If a potential is applied across

---

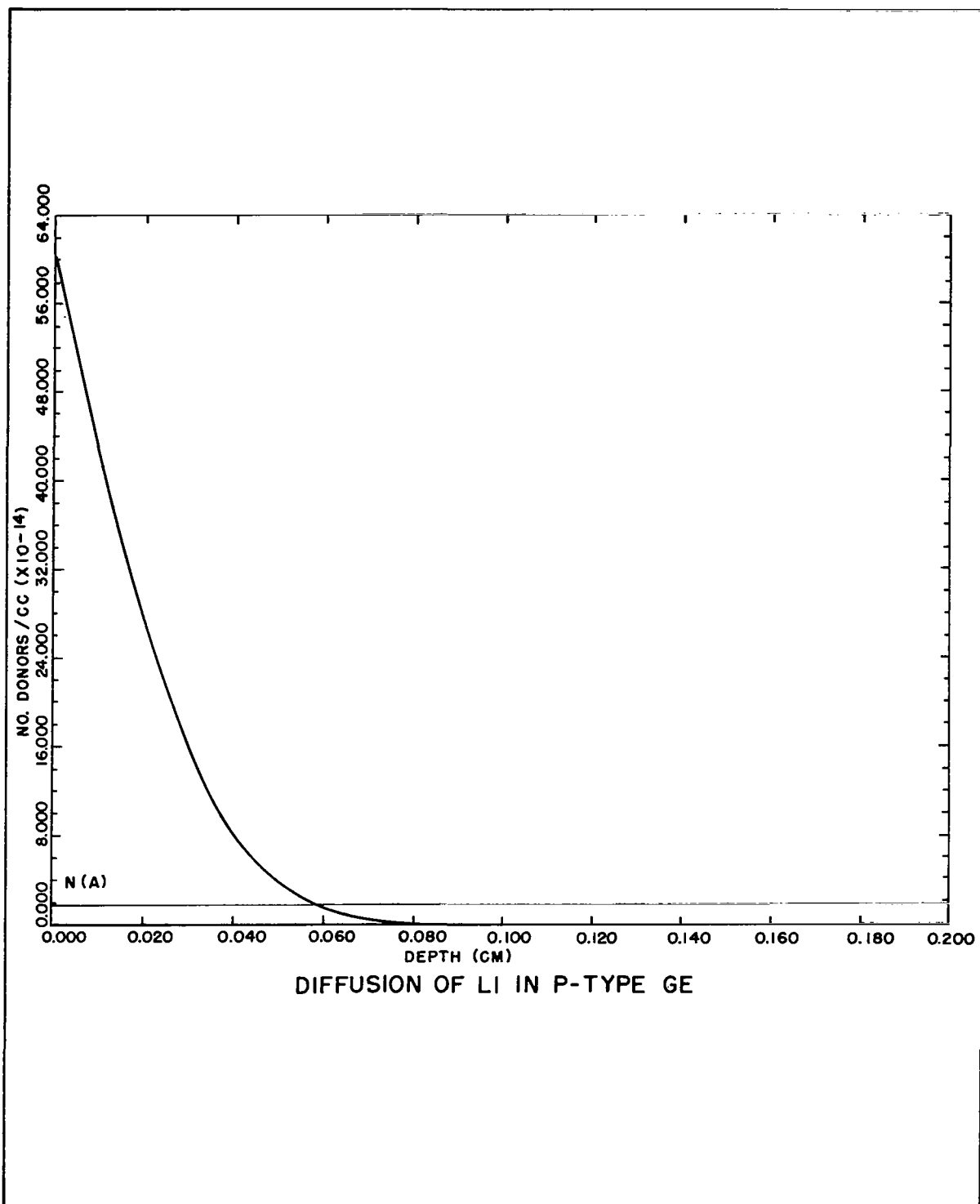[*]Carslaw and Jaeger, Conduction of Heat in Solids, Oxford University Press, (1959), p. 60.

Figure 3. Acceptor and Donor concentration vs. depth;
following lithium diffusion into germanium.

the crystal after the diffusion, the electric field will be applied almost in its entirety at this point called the "junction."

2. Lithium in Germanium Solution

Unfortunately, lithium is relatively insoluble in germanium. The solubility of lithium in germanium is roughly exponential with temperature[20]. The equilibrium concentration of lithium at $425^{o}C$ is about 6000 times that at the temperature normally used for drifting, resulting in a supersaturated solution[20]. It is inevitable that the lithium in such a condition will precipitate. The seriousness of the situation will in general depend on the time taken to fall below the concentration needed to fully compensate the initial acceptor density. The lithium loss as a function of time has been measured by several authors[20-22], and it appears that within three hours after the diffusion the lithium concentration will fall to about 1% of its initial value. A measure of the seriousness is the net carrier density in the region that is depleted. Measurements have shown[23] that well-compensated material with a net acceptor density of approximately 10^7/cc will exhibit an increase of two orders of magnitude in acceptor density in the first 100 hours at room temperature. It is certain that the precipitation of lithium is directly related to the mobility, as the lithium will have a tendency to precipitate at nucleation centers of several types and must therefore move from a somewhat homogeneous distribution to a distribution of agglomerates[21]. By reducing the mobility of the lithium ion, primarily by restricting the temperature, the precipitation is virtually checked at $77^{o}K$. This is of course an automatic outcome of operation at minimum noise, but during the drift process, to be described in the next section, the temperature is necessarily elevated to encourage high mobility.

There are two methods in current use to restore the original lithium

concentration. The first is simply to reheat thereby redissolving the agglomerate lithium and to continue the drift from there. The other method is a straightforward elimination of those nucleation sites at which the lithium tends to condense. Copper is known to have a much higher mobility in germanium than lithium[24]. Therefore, if copper is pre-diffused on the germanium to make a supersaturated copper solution, then upon cooling, the copper, with its higher mobility, preferentially seeks out the nucleation sites and blocks the local gradients that attract the lithium to these catalysts. The copper apparently has no further effect on the drift process[25]. Other materials such as nickel have been tried in an attempt to achieve the same effect with uncertain success*. It is the opinion of the authors that the prediffusion has not shown itself to be worthy of the difficulty it entails. Redissolving the lithium will, of course, increase the possibility of introducing impurities as well[26]. If the initial material is of sufficiently high quality, rediffusion or copper diffusion should not be necessary as precipitation will be no problem.

3. The Drift Process

    a. Principles

        The object of the drifting process, previously explained, is to induce lithium to impurity sites so that it forms ionic bonds and compensates. Whereas lithium is a large atom, it is a small ion and under the influence of an applied electric field it readily moves interstitially through the germanium lattice. When it is attracted to, and bonds with the acceptor site, it loses its ability to respond to the electric field in this manner. It can be shown that the resulting distribution from such a situation is a

---

*G. Dearnaley, Private Communication, March 31, 1965.

14

stable one and will result in the lithium being implanted in such a way as to make the material that can be reached in any given time appear to be intrinsic. Pell[19] has shown that after the transients of the problem have disappeared, the width of the lithium-compensated region will vary as

$$W = \sqrt{2\mu V t / RT}$$

in a crystalline field,
where

W = depth of drift	t = time
μ = mobility of Li	k = Boltzmann's const.
V = applied voltage	T = Absolute temperature

Several convenient nomographs have been prepared which facilitate depth estimates[27].

Unfortunately, the interstitial lithium performs the compensation so effectively that it has the tendency to compensate the average charge density that is present due to leakage current from the reversed biased diode. The current, which can be as much as $40mA/cm^2$ during a rapid drift, can cause the crystal to be seriously overcompensated. When the crystal is cooled and the lithium is no longer free to move it is frozen in this overcompensated state and may produce an intolerable bulk leakage current during operation. The relation for lithium distribution generated by such conditions is derived in the Appendix for planar and cylindrical geometry.

In order to reduce this overcompensation to a tolerable level (it can not be completely eliminated) a post "cleanup" drift is often carried out. There are several techniques to accomplish this, and the most important of these will be described in the section relating the fabrication techniques used in this work.

b. Cylindrical Drift

The most obvious difficulty in fabricating a large volume diode is to drift a depth deeper than 1 cm. Either enormous amounts of power must be applied to a temperature-regulated crystal or the drift must be extended for several weeks. The disadvantage of extending the drift time beyond two to four weeks is that precipitation of the lithium will become a serious problem. Furthermore, when the depleted region is extended to a depth greater than, say, 1 cm, the problem of complete charge collection becomes important. Extending the area of the diode in order to increase the active volume can only be done at the expense of increasing the junction edge area. As the junction edge is the most vulnerable surface to contamination, this is not an ideal manner in which to expand the volume[28]*. Furthermore, carried out to any extent, it results in ungainly shaped detectors.

Many of the above problems are less serious if the diode is made in the form of an annular cylinder. Three such cylinders were made as part of this research project with dimensions 1 inch diameter by 1 inch long with a 3/16 inch hole bored through the axis. The lithium-n surface was made the outer curved surface and the gallium doped germanium-p contact was made to the inner curved surface. The junction "edges" were the two annuli on the cylinders' ends. The fabrication methods for such detectors will be discussed in the next section.

The advantages of this geometrical form are numerous. The most obvious improvement of such a geometry over the planar is that in the same drift time to compensate a given depth with the planar geometry, the cylindrical geometry produces, with a comparable depth, a virtually unlimited volume, merely by

---

*A guard ring structure can be used to reduce noise from edge leakage current. See also (29).

extending the length. The only limiting factor in this respect appears to be the uniformity of available crystals. The crystals that are currently available have a forbidding nonuniformity over a length of roughly 20 cm. As the volume is increased by lengthening the cylinder, the junction geometry remains unchanged. The junction edge area is likewise unchanged, so that the leakage current across this junction surface would not be expected to change.

Any method that increases volume would be a great sacrifice if it did not result in an easily measurable and calculable geometry. Furthermore, the geometry should be easily reproducible so that calibrations made for one series of detectors could be applied with little or no modification to any other set. The annular geometry is convenient to such standardization, but no other proposed or produced detector satisfies this important criterion.[*]

The axial hole provides an added feature besides the utility of a center contact; the dead material that would only serve to scatter Compton electrons into the active region is missing, and so the Compton background is reduced.

It is known that material defects in the form of dislocations can act as nucleation centers for lithium, thereby adversely affecting the drifting process in those areas[34,35]. Furthermore, the mobility of lithium seems to be appreciably greater in those regions that exhibit high dislocation counts. If the drift direction were in the same direction as "grain" produced by such ribbons of damage, then the difficulty known as "punch-thru" is prone to

---

[*]"Coaxial" detectors have been produced at other laboratories by drifting from five sides of a piece of a germanium[27,30-33]. This results in a very large volume detector, with published volumes up to 45 cm^3. The serious difficulty presented by this method of drifting is that the shape of the active volume is highly irregular and very difficult to measure. The wide variation in collection field and the resulting variation in pulse shape, make it unsuitable for fast timing experiments.

occur[*]. Measurements made by a major producer of germanium[**] convincingly indicate that the grain of the dislocations is in the direction of crystal length and is concentrated strongly at the center and at the crystal edges. Figure 4 shows a dislocation mapping of one of the crystals as prepared by the supplier. It is quite clear that the center location "5" consistently has the greatest dislocations of the cross sectional area. A,,B,C,D refer to four cut surfaces of the ingot.

In the cylindrical geometry the drift is perpendicular to these ribbons of dislocations, and furthermore, the largest concentration of dislocations, at the center, are removed as the central core.

C. Fabrication Techniques

During the few years that lithium-drifted germanium detectors have been made, there has evolved an enormous array of taboos, some with merit and some perpetrated through ignorance. It is hoped that the number of unexplained schemes can be reduced in the following discussion, although all of them cannot be eliminated. It is for this reason that the fabrication of Ge(Li) detectors must at this time be referred to as an art.

1. Summary of Fabrication Procedure

The cylinders are cut from the standard Sylvania #4 ingots, allowing a maximum outside diameter of one inch, as is shown in Figure 5. The shell left after the cored cylinder has been removed is shown next to the cylinder. All the detectors made to date have had 3/16" diameter holes cut concentric with the outer wall.

_____

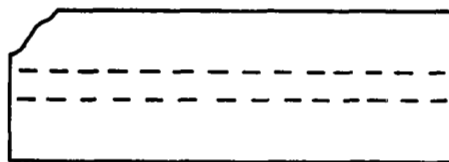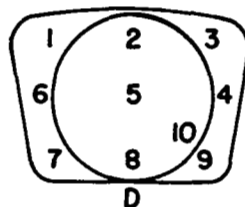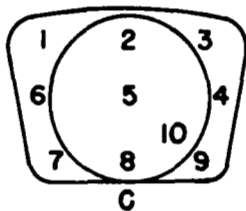[*]G. Dearnaley, Private Communication, March 31, 1965.
[**]Sylvania, Towanda, Penn.; measurements made by P. Stermer, Private Communication.
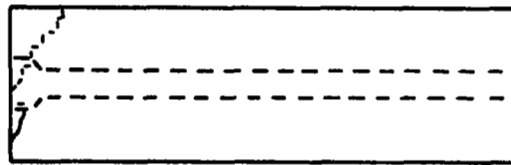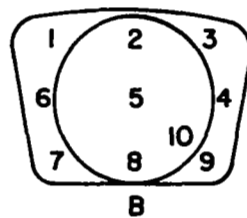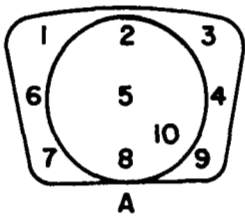
NO.	A	B	C	D
1	22	27	18	24
2	10	13	17	11
3	18	19	13	22
4	9	9	10	8
5	40	51	36	32
6	17	22	24	9
7	8	10	9	11
8	5	5	6	5
9	9	15	12	20
10	8	9	14	10

ALL READINGS X 100

FLAT AREA   LOT# 655F-3

LOT # 637G-2

Figure 4.   Dislocation mapping of a cross section from
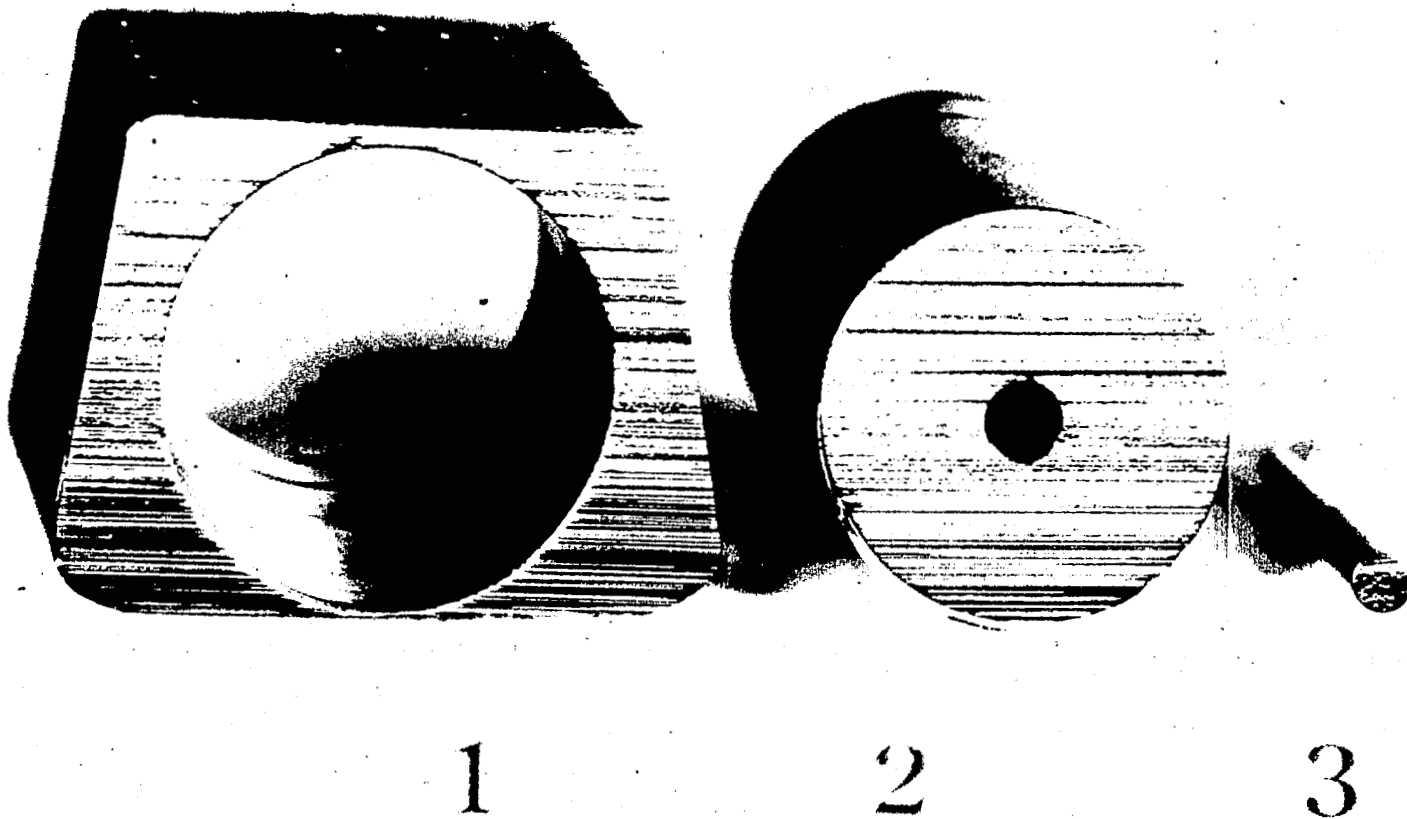a germanium ingot (Sylvania, Towanda, Penn.).

Figure 5. The coaxial annulus is spark cut from the standard Sylvania #4 ingot. The two concentric cuts leave a shell as shown on the left and a core shown on the right.

The forming of the annular shape from the germanium ingot is done by spark cutting[*]. We initiated the application of spark cutting in detector fabrication because damage to the germanium crystal is slight as contrasted with that caused by grinding and polishing[**]. The first four crystals were cut by Sylvania[***] with only the center hole spark cut. We now spark cut all the surfaces ourselves. The cutting of the inner and outer cylindrical surfaces is shown in Figure 6. The cutting tool is a molybdenum tube, one inch diameter for the outer cut as shown on the right and 3/16" diameter for the inner as shown on the left. We found that the cutting speed is increased if the tubes are rotated at approximately 150 r.p.m. during the cutting. (A continuously moving wire spark slicer is used to trim the flat surfaces, which are the junction edges, after lithium diffusion.)

The lithium is then evaporated on the outer surface and drifted radially toward the inner cylindrical surface. As a result of this method we obtain an annular intrinsic region whose length is well known and whose thickness can be determined by capacitance measurement or copper staining. The detector has a relatively large, well defined sensitive volume with little dead volume.

2. General Preparation

Cleanliness is perhaps the most important rule, and any dust or condensable vapor that might contaminate the surfaces, especially the junction surface, should be avoided. This becomes increasingly more important as the detector nears the latter stages of completion. Soldering should not be

---

[*] The spark cutting machine is commercially made by Metals Research Ltd., Cambridge, England.

[**] J. W. Mitchell, Private Communication.

[***] Sylvania Electric Products, Inc., Towanda, Pennsylvania.

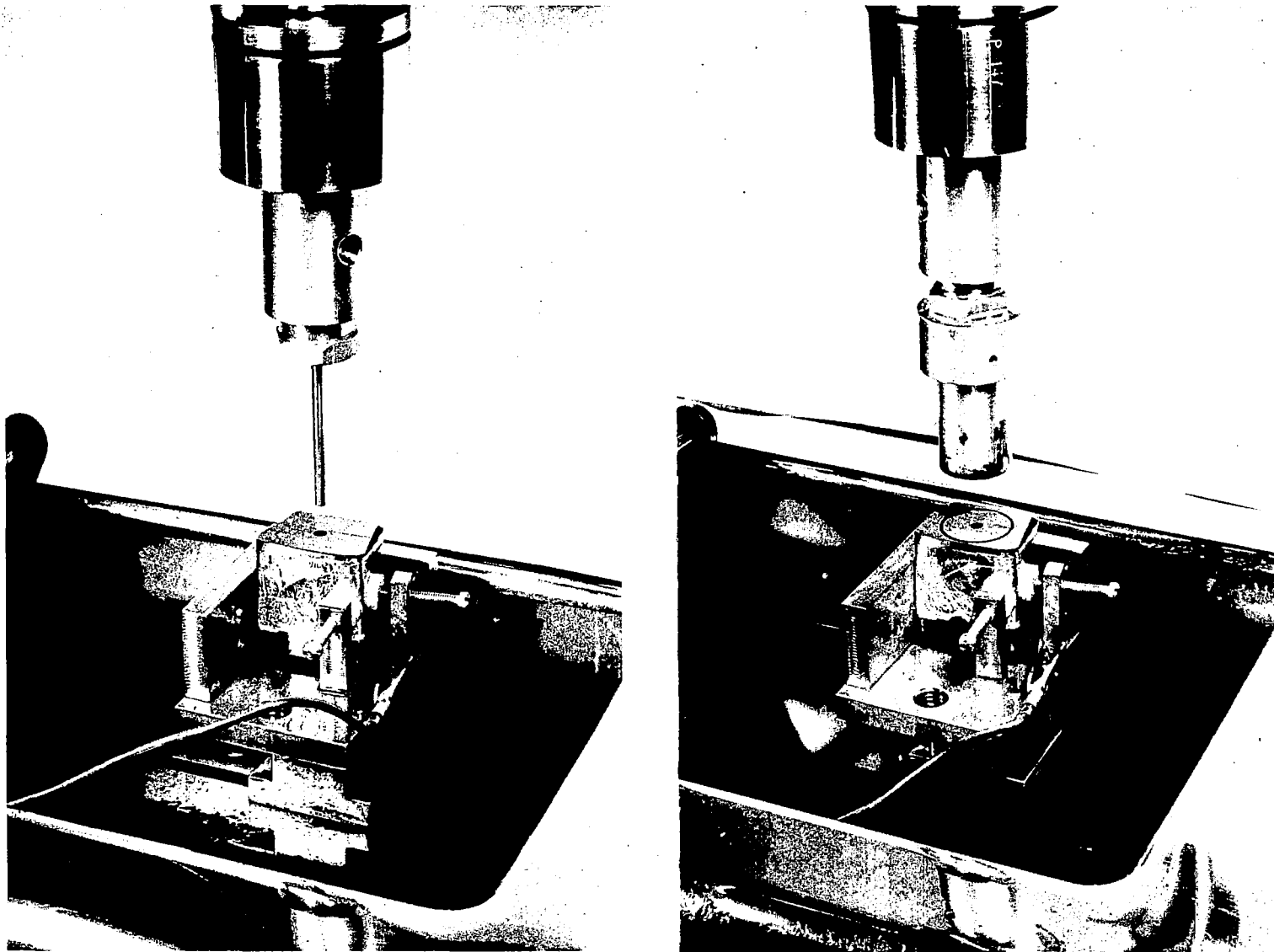Figure 6. The annulus is spark cut using molybdenum tubular tools. The inner (3/16 inch diameter) hole is partially cut at left; the other (1 inch diameter) at left. The tool is rotated at 150 r.p.m. while cutting.

carried out in the same room in which the detectors are made, at least for a couple of days before the crystal is to be exposed. Smoking should be avoided in the room in which the detectors are to be made. There are many other condensable vapors that will be difficult to remove and any heavy vapor should be avoided if its nature is unknown.

All chemicals should be the purest obtainable, especially those used for the etch. The chemicals used in this work will be indicated when introduced. The chemicals that are to be given the most attention are those that are used in the final states. They are:

Methyl Alcohol: The methyl used in this experimental work was Fisher 99.9 Mol% Pure (A-936). It does not cost much more than the utility methyl and relieves this solvent, which is used commonly, from suspicion of contamination. In general Ethyl is not a good substitute for Methyl since its purity is hardly ever stated.

Distilled Water: The water used for the washes and in mixing acids should have a resistivity greater than 1 megohm-cm. This corresponds to an impurity concentration of less than 1 part in 10 million of ionizable salts. This will not be realizable unless the water is deionized and demineralized just prior to use. This can easily be accomplished by using an ion-exchange resin type of demineralizer and using this water directly without storage for the final rinses.

Chemical Polishing: The most suitable etch for germanium is CP4[36-38] which is prepared as follows:

> 2 volumes conc. nitric acid (A200 Fisher) 70%
>
> 1 volume Glacial Acetic Acid
>
> 1 volume 48% HF (A-147)

This should be mixed in clean polyethylene apparatus and allowed to stand for

30 minutes before use. A new batch should be mixed for each days use. If etch pits appear when the specimen is etched, then it may be necessary to substitute Fuming Nitric Acid for the Nitric specified. Fisher A-202 has been used for this purpose (90%). Polyethlene gloves are recommended when handling these acids.

3. Detailed Fabrication Procedure

   a. Initial Cleaning

      The sample that is to be diffused and drifted should be absolutely free of surface contaminents at the very beginning so that in the initial diffusion these impurities do not penetrate the surface and cause deleterious reverse-bias characteristics when the drift is initiated. This can best be carried out by:

      1. Immersion in Chromic Acid (made by saturating concentrated sulfuric acid with sodium dichromate) to remove organic impurities. The use of an ultrasonic vibrator will be of great help to loosen caked material.

      2. Rinse with distilled water.

      3. Immerse in hot concentrated nitric acid for 5 minutes. Use ultrasonic vibrator.

      4. Rinse with deionized water. NOTE: (whenever germanium is in acid and is to be removed, the acid should be repeatedly diluted and decanted until the germanium is in nearly pure water, and then transferred to a clean beaker with fresh water. Never bring a germanium surface directly from an acid into air contact.

      5. Etch in CP4 until the surface of the crystal appears uniformly clean. It is important to keep the acid swishing constantly during all etches

so that the bubbles do not insulate the surface from the etch. Do
not use the ultrasonic vibrator, in general, during etches as this
appears to accelerate the formation of pits.

6. Dilute and decant until the crystal can be removed from the etch
    and transferred to a clean beaker and wash several times with fresh
    deionized water. A separate beaker should be set aside for this
    final wash and used for no other purpose.

7. Dip the crystal into methyl and place onto clean filter paper to dry.
    Drying may be accelerated by playing a stream of clean dry nitrogen
    on it.

b. Lithium Diffusion

It was suggested[*] that the cleanest way to apply the lithium
to the surface of the germanium is to evaporate in vacuum. This is preferred
to the method of painting the lithium-in-oil suspension as it eliminates the
problem of disposing of the oil or kerosene. The lithium used here is reactor
grade purchased from Foote[**] in 1 pound ingots. It is stored in a vacuum
dessicator with silica gel, the dessicator being kept in a glove box filled
with argon. When it is necessary to remove some lithium for evaporation, the
glove box is flushed with several volumes of argon and a small, steady flow
is maintained to assure a positive pressure inside. A small amount of lithium
is cut from the ingot after an area of the ingot is scraped clean of scale
and immediately placed in an argon-filled plastic bag. The bag is knotted
shut. Argon was used mainly because it was conveniently available, but dry
nitrogen is to be preferred for lithium handling.

The apparatus for evaporating and diffusing cylinders is shown in Figure

---

[*]A. J. Tavendale, Private Communication.
[**]Foote Mineral Company, Paoli, Pennsylvania.

7(a) and 7(b), and a schematic of the oven is shown in Figure 8. The crystal (A), is supported on a thin-wall stainless tube. The wall thickness of the tube has been reduced as much as possible so that heat losses through conduction are minimized. The crystal is restrained from sliding by two small molybdenum cups, that are in turn restrained by fine slits in the stainless tube. The stainless tube is fastened to a stainless rod that is supported by bearings and turned by a small synchronous motor at 120 r.p.m.[*]. The motor is suitable for operation in vacuum for short periods of time. The shaft has three circular molybdenum heat shields that turn with it, one inside the oven and two outside. There is an additional shield that protects the bearing assembly from the radiated heat, (Molybdenum heatshields are designated "M" in the diagrams). The oven is made from McDanel High purity alumina[**] (B), cut to a length of 4 inches and a 1.5 x .5 inch slot cut in the center. The slot allows evaporating lithium to pass into the oven for deposition on the germanium. The oven is wound with a tungsten coil and cemented in place with McDanel AV30 alumina cement, and fired at $3000^{o}F$. The whole oven is contained in a copper housing and supported on alumina rods (R) (shown schematically). There are two concentric molybdenum cylinders and two end sheets for heat reflection. The copper housing is water cooled (W). The motor and crystal assembly is on a track and can be withdrawn from the oven using a mechanical vacuum feed-through. The oven was calibrated using a germanium cylinder identical to those used for drifting except that two small holes were bored (using the spark cutter) near either end and two thermocouples inserted with a small amount of indium for thermal contact. The calibration is shown in Figure 9.

---

[*]Purchased from Hayden Clock Company, Waterbury, Conn.

[**]Purchased from McDanel Refractory Porcelain Co., Beaver Falls, Pa.
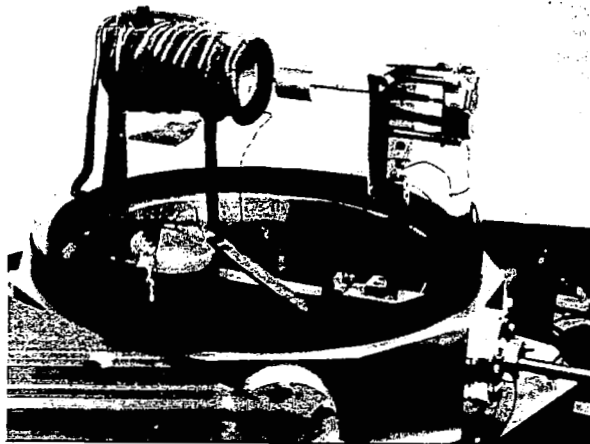
Figure 7a. Cylindrical oven for evaporation and diffusion of lithium.
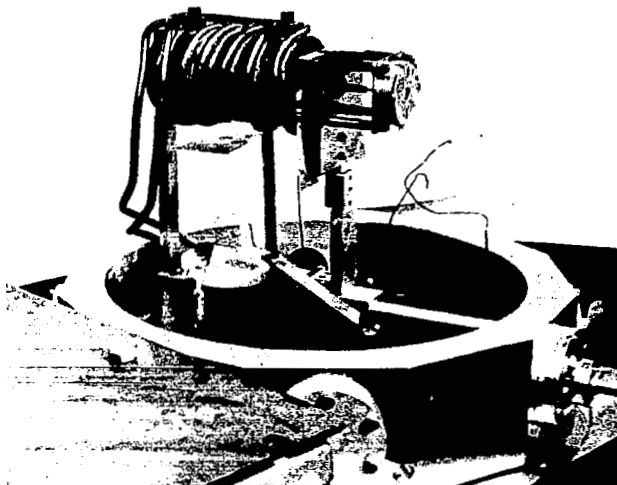Crystal and motor drive assembly are shown retracted.

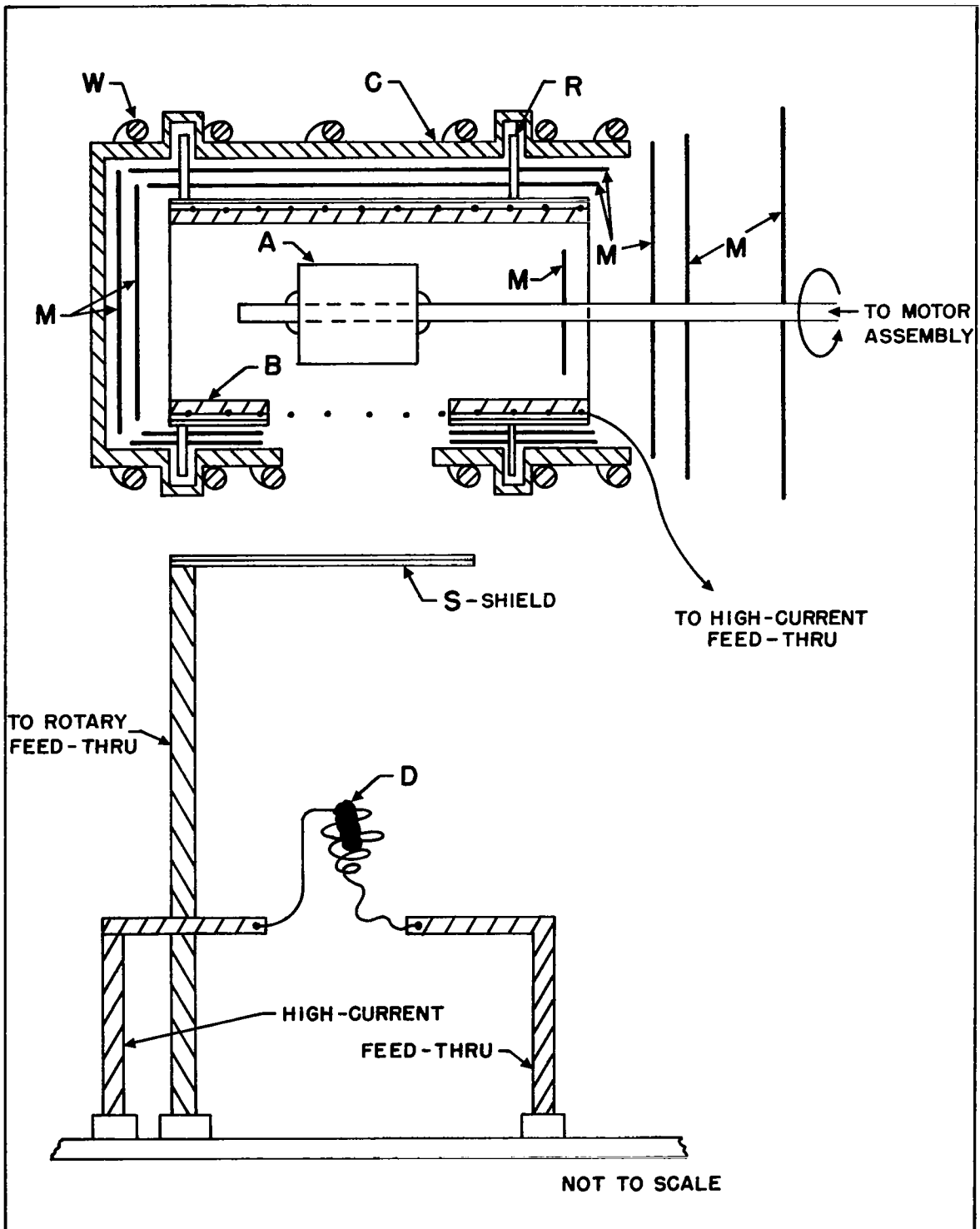Figure 7b. Cylindrical oven with crystal in position.
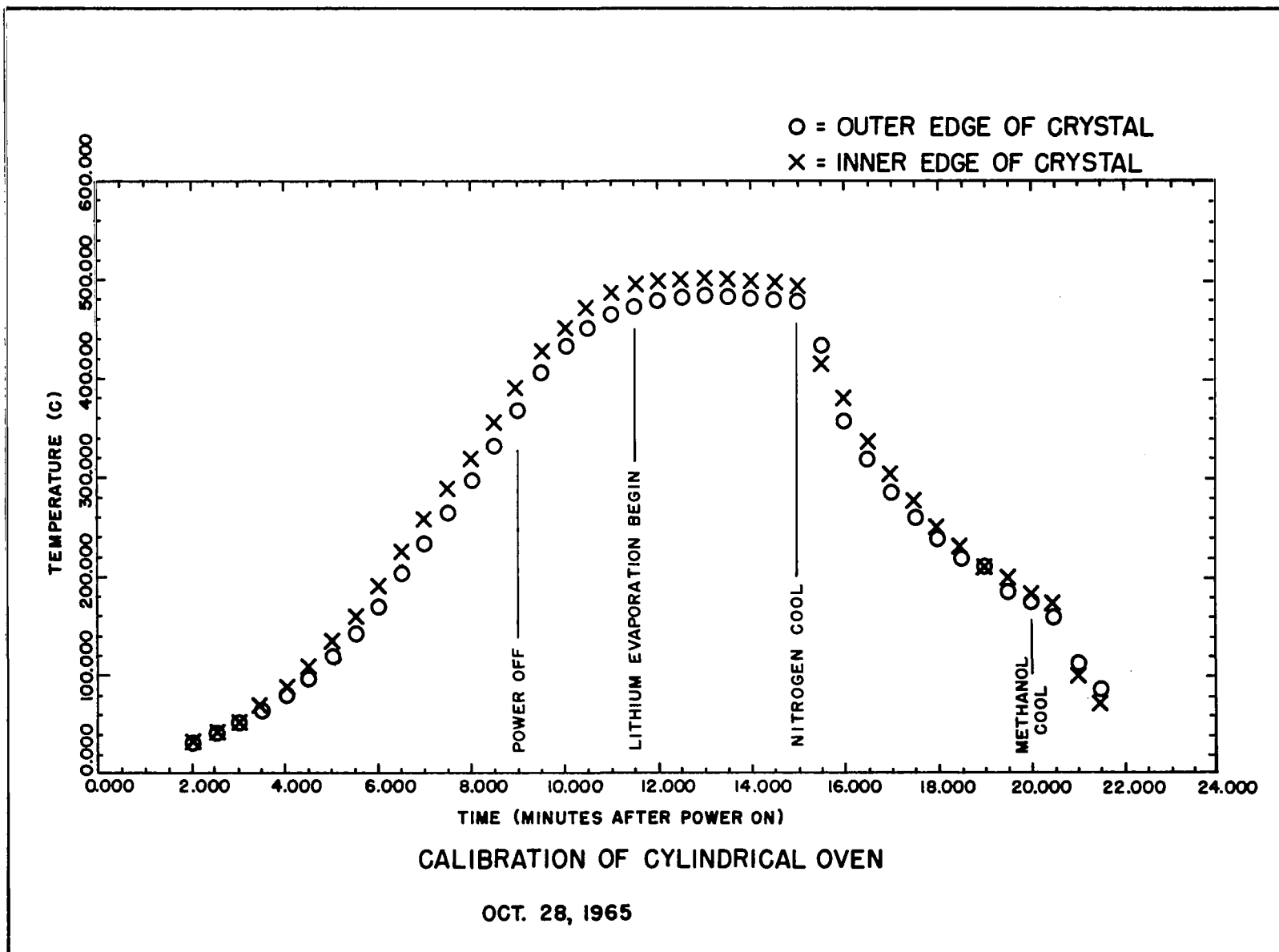
Figure 8. Diagram of cylindrical oven.

Figure 9.   Temperature calibration of cylindrical oven during diffusion vs. time.

In operation the procedure is as follows:

With the flag, (S) in place so that no lithium may enter the slot, the lithium is warmed to the melting point by heating the basket filament (D). This will allow any volatile impurities to boil off before evaporation begins. The filament is then cooled slightly so that the rate of evaporation is negligible. The oven is turned on by applying 30 volts (240 watts) slowly at first, until the tungsten resistance stabilizes. After 8 minutes the power is raised to 300 watts (40 volts) and one minute later, 9 minutes after start-ing, the power is shut off. As the calibration shows, the oven will coast up to 480°C and during this time the lithium should be starting to evaporate. At 11 minutes to 15 minutes, the flag is turned aside and evaporation and diffusion are maintained simultaneously. At this time the lithium should be evaporated as fast as can be done without sputtering. The lithium will, of course, short the tungsten wire reducing the power transfer but this should present no serious problem.

At 15 minutes after starting (a total diffusion time of 4 minutes), the following are performed quickly in succession:

1. the evaporation filament is turned off,

2. the crystal is withdrawn from the oven,

3. the vacuum valve is shut, and

4. super-dry nitrogen is quickly bled into the system to cool the crystal rapidly.

This will result in the maximum supersaturated lithium solution. After 5 minutes of nitrogen cooling, the system is opened and methyl is cautiously dripped on the spinning crystal being careful not to shock the crystal thereby cracking it. This is done until the crystal is cold.

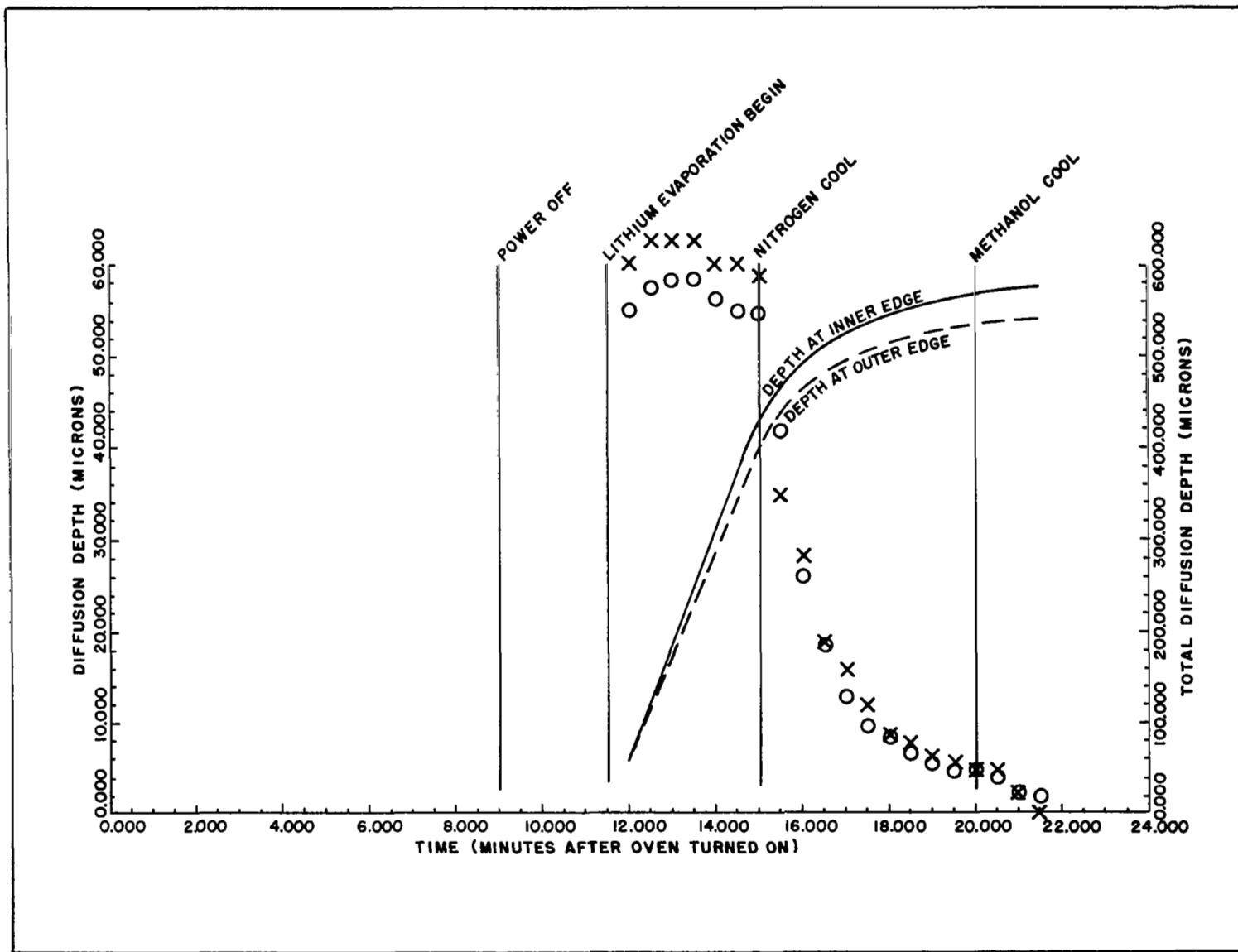Figure 10 shows the differential and integral diffusion depth as calculated

30

Figure 10. Differential and integral diffusion depth vs. time.

from the diffusion constant of lithium in germanium[*]. Since the diffusion

constant is varying exponentially with temperature, extreme care must be

taken to assure that the temperature is known over the entire crystal volume

so that uneven or excessive diffusion is avoided. The total diffusion depth

as calculated (Figure 10) is shown to be 540 and 562 microns on either end of

the crystal. Subsequent measurements on a cylindrical sample showed the depth

to be 550 $\pm$ 25 microns on both sides as made visible by spark cutting and

copper staining (both to be described below). The crystal is now removed

from the mounting and washed in methyl followed by water, and again in methyl

to remove excess lithium from the surface. The flat ends of the crystal are

removed by slicing with the wire spark cutter (or diamond saw if spark cutting

is unavailable) so that there is no chance of lithium being present on the

junction surface.

c. Spark Cutting

The use of the spark cutter for all germanium cutting was

initiated for the following reason: cutting with a diamond saw leaves a

damaged layer which is quite deep and extremely variable, depending on the

cutting rate and the condition of the blade. The subsequent polishing and

lapping by abrasive is only effective if it completely removes the initial

damage and is done in careful successive grades to a final lapping with micron

alumina. The termination of the abrasive polishing is so subjective that re-

producible results are difficult to attain.

The slicing by means of a spark cutter, on the other hand, does not pro-

duce damage beyond a few microns into the crystal[**]. The actual extent of

---

[*]Values for diffusion constant of Li in germanium given in (39), p. 186. See
also (40).

[**]J. W. Mitchell, Private Communication.

damage has yet to be measured, and a program is under way at this writing to undertake such measurements. A good indication of the damage produced by any method of cutting germanium is to observe the bubbling that accompanies the etch. The damaged germanium (i.e., polycrystalline) etches at a much more rapid rate than the single crystal and the specimen will bubble profusely while there is still damaged material being removed.

The actual spark cutting instrument is commercially made and the cutter attachments were made in this laboratory. The cutter wire, 0.0015" molybdenum, is drawn over two pulleys from its original spool onto a clock motor-driven drum. The specimen and the wire cutter are immersed in kerosene while the servo-control in the device maintains a gap sufficient to discharge a selected capacitor through the kerosene, to the specimen. There is no mechanical contact with the crystal, and due to the kerosene there is no surface heating.

d. Preparation for Drifting

The crystal must again be cleaned thoroughly.

1. Immerse in trichloroethylene after the spark cutting and agitate with the ultrasonic vibrator. Remove the crystal to a second beaker of "trico" and repeat the above. (Note that it is important to use polyethylene beakers for the ultrasonic cleaner. Whereas glass, being rigid, couples very well to the ultrasonic vibrations, it is too hard and the germanium, rattling around, tends to chip at the sharp edges.) Continue to use fresh trico until the solution does not darken with carbon.

2. Wash in methyl twice.

3. Dip into water to wet the surface (so that the etch attacks evenly).

4. Etch until the surface stops bubbling. It may happen that the heat generated by the etch is enough to cause the etch-rate to become too high and "run away", thereby forcing the etch to be terminated prematurely. This may

be avoided by cooling the etch, but it is preferable to have a second quantity on hand. It is not possible to remove the crystal from the etch since it must be diluted and decanted. Otherwise rapid oxidation of the surface will take place. At this point the surface condition will influence the initial drifting characteristics and care should be taken to have a clean, unpitted surface.

5. Dilute and decant with water.

6. Remove from decanted "acid beaker" to the "wash beaker" and rinse several more times.

7. Dip in, or squirt with methyl (a drying agent).

e. Drifting Apparatus

Two methods of drifting have been used, with equivalent results except for drifting time. They differ only in the ambient and its effect on the cooling. The first method takes place in a dry nitrogen gas atmosphere. The crystal cooling is accomplished by water circulation in the blocks that hold the specimen and apply the bias. The apparatus is shown in Figure 11.

The positive voltage is applied to the outside block via the copper tube from the outside, and the inner tube is grounded. Cold tap water is circulated through both halves of the outer copper blocks, passing through a labyrinth inside for maximum heat transfer. The inner tube conducts water that is electrically isolated from the high-voltage water by several feet of plastic tubing, thus the crystal is cooled at both n and p surfaces. The boss on the front side of the outer block is a thermocouple connection. To mount the sample in this apparatus, the crystal is first wrapped in a layer of indium foil, and the inner tube is wrapped with indium foil. The crystal is slid over the foil-covered tube, making a snug contact, and the outer blocks are placed around the crystal and fastened together with a strong spring, thereby
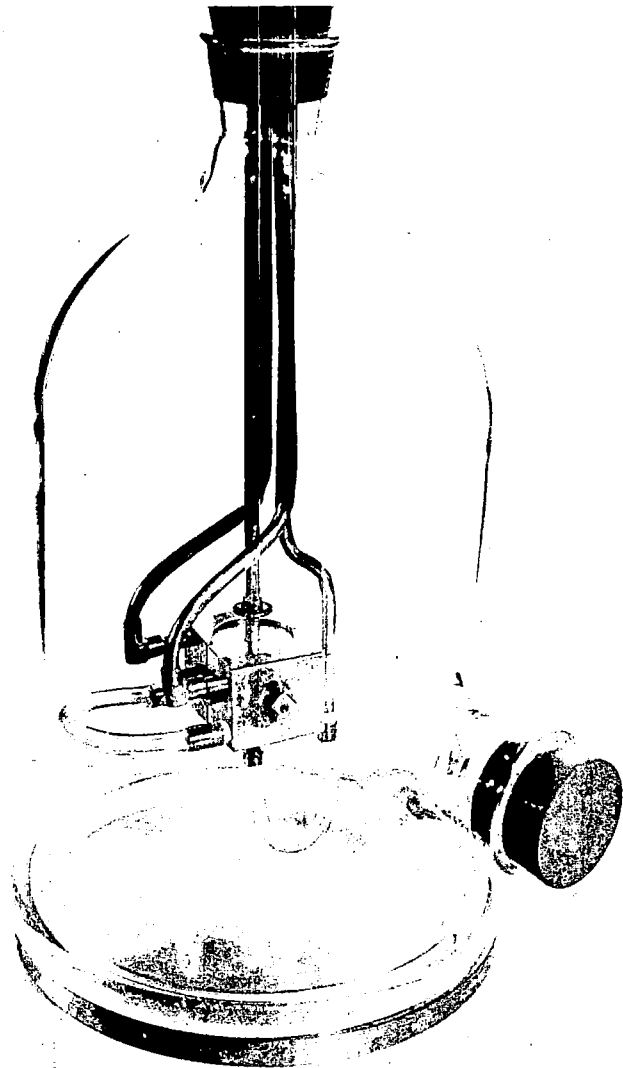
Figure 11a

Figure 11b

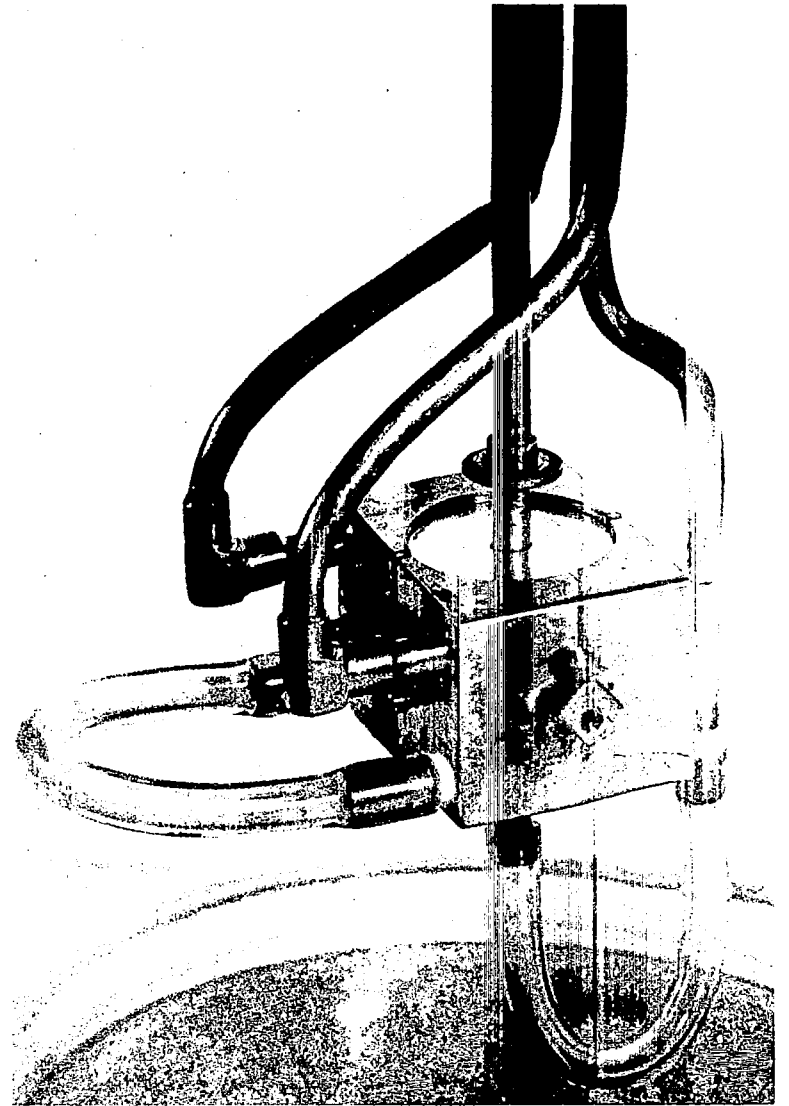Drifting apparatus. Copper blocks are water cooled; ambient is dry nitrogen.

allowing for expansion and contraction.

The characteristics of the gas ambient drifting apparatus is described in this subsection rather than in the one following denoted "drift procedure" because it is believed that the liquid-cool method is superior from several standpoints and should be described in somewhat more detail.

At the onset of drifting, the chamber is evacuated to 1 micron or better (evacuation is through side stopper, connections not shown) and flushed several times with dry nitrogen. The drift was originally carried out in the vacuum, but direct comparison of the diode characteristics for the two ambients showed that dry nitrogen was a superior choice. The data is exhibited in Figure 12. It is believed that different gases affect the surface states of germanium in markedly different ways, and that this is a possible explanation of the effect.[*] There is undoubtedly a contribution to the difference caused by dissimilar heat transfer at the junction surface. Data taken in the above-mentioned figure was repeated several times.

When the diode begins to deteriorate, the nitrogen is pumped out of the bell jar and the crystal allowed to warm slightly (by shutting off the cooling water). The previously "good" characteristic is restored when clean nitrogen is reintroduced. The drift voltage at constant current has repeatedly been raised from around 220 volts to about 350 volts in this manner.

    f. The Drift Procedure

        The apparatus for drifting with liquid cooling is shown in Figure 13(a) and 13(b). The schematic diagram shown in Figure 14 shows the manner in which the crystal (B) is mounted. The crystal is wrapped with a layer of cleaned indium foil (C) to serve both as a cushion and as a n-contact.

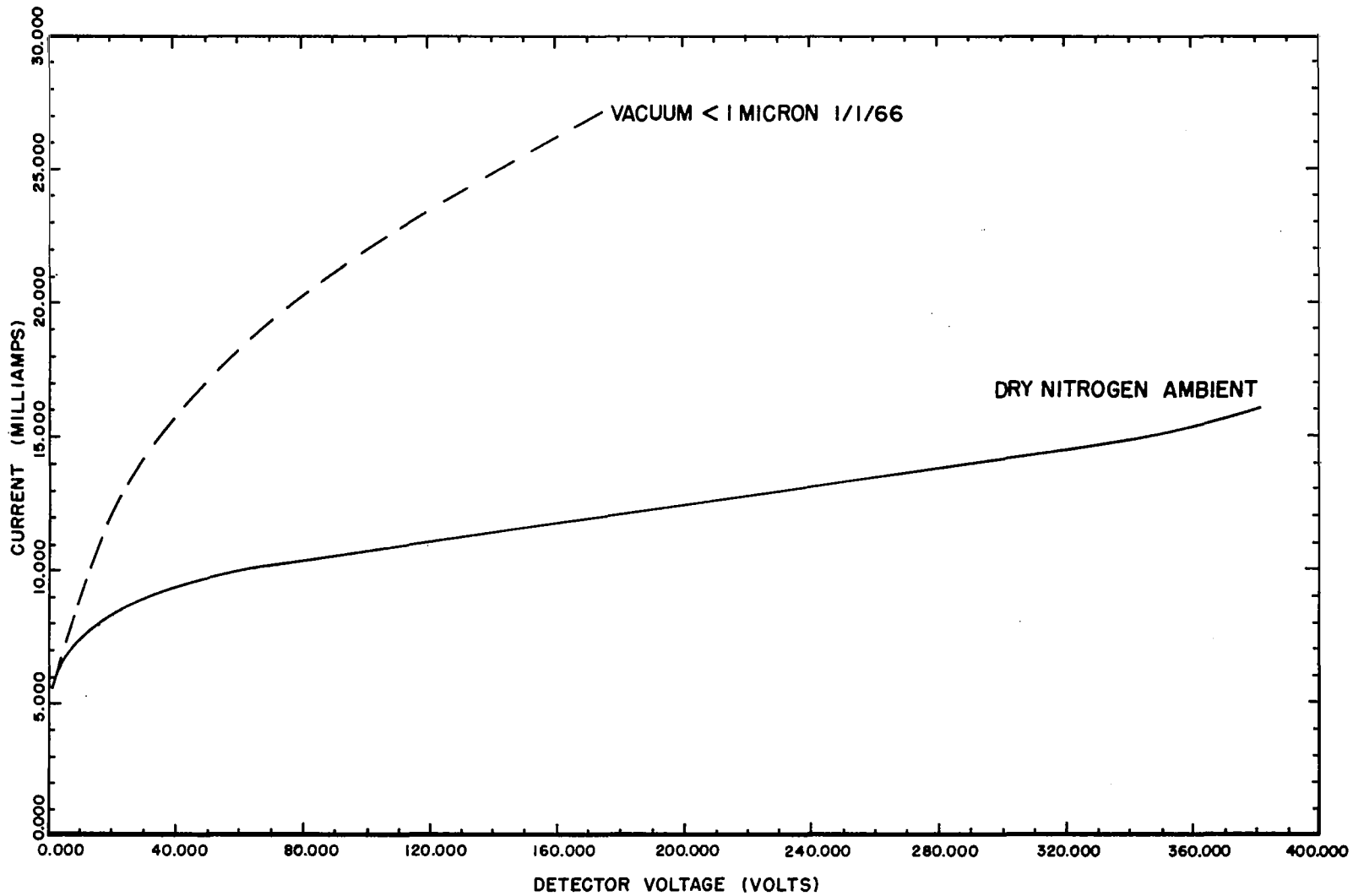[*] F. Goulding, Private Communication, January 7, 1966.
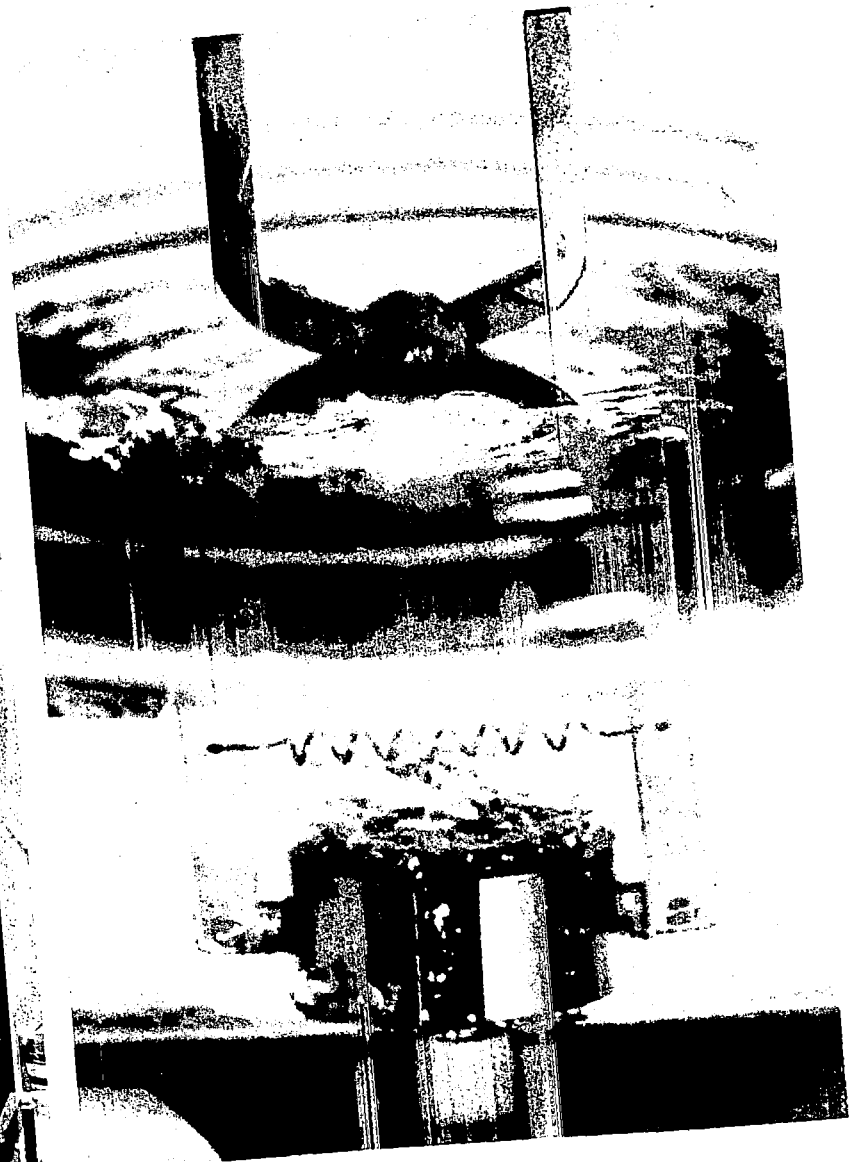
Figure 12. I-V Curve

Figure 13b

Figure 13a

...aratus: a) overall view showing complete apparatus, b) closeup view during drifting shows
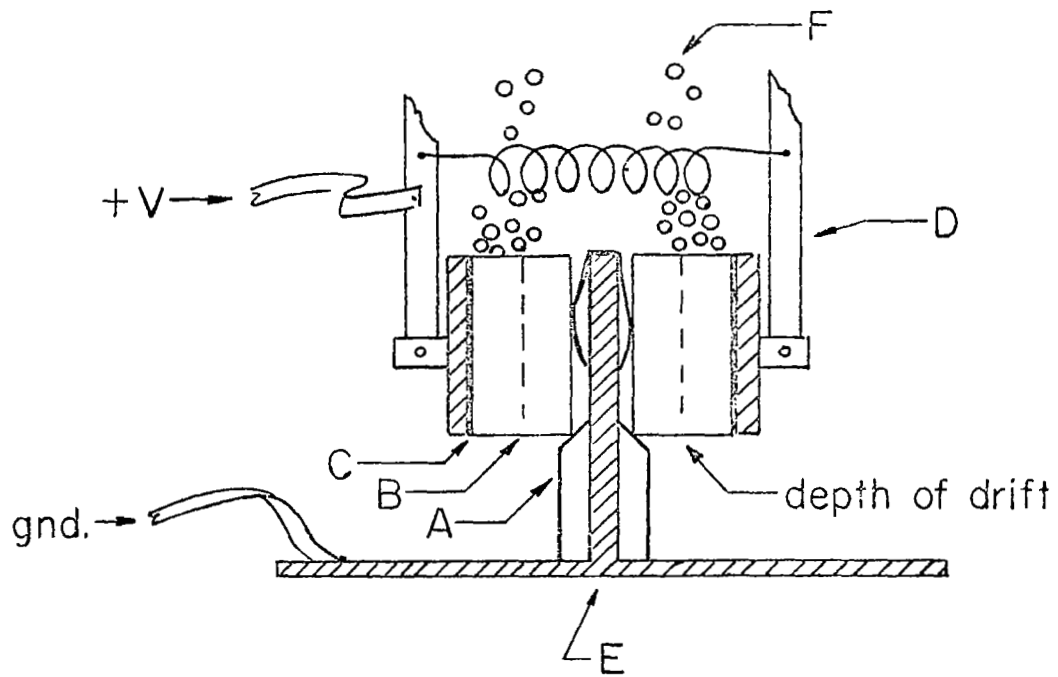
38

Figure 14. Diagram of boiling Freon drift apparatus.

It is picked up with the (gold plated) copper clamp (D) and held by a strong spring. Positive bias is applied to this clamp. The crystal is placed onto a spindle-platform (E), with the grounded contact being made via a gold leaf spring, and lowered until its edge rests on a teflon support (A). The container is filled with a non-polar liquid and sealed. Freon TF cleaner* has been chosen for this purpose since its boiling point, $47^{\circ}C$, is close to, but comfortably below the point at which the thermally-generated carriers make the p-type germanium intrinsic. The condensing column allows refluxing of the freon boil off. When bias is applied, the heat transferred to the freon causes it to boil. The boiling is fairly localized to the region already depleted (F) as can be seen in Figure 13(b).

The drift process is as follows:

1. Nickel plate electrodes onto the germanium crystal. The electroless method[41] is used to plate the entire surface of the cylinder. The process uses a solution of

Nickel Chloride	30g/l
Sodium hypophosphite	10g/l
Ammonium citrate	65g/l
Ammonium chloride	50g/l

The solution is filtered twice and ammonium hydroxide is added until the solution turns from an emerald green to a deep blue color. The solution is raised to $95^{\circ}C$, and the crystal immersed for about 40 minutes after solution resumes boiling. This results in a nickel thickness of approximately 7 microns. Carefully remove the crystal from the plating bath; the solution is apt to make the crystal slippery and precarious to handle. Wash in water.

---

*Purchased from Dupont, Wilmington, Delaware.

2. The nickel must be removed from the flat surfaces. The outside contact is covered with solvent resistant polyester tape ("Scotch" #853) and trimmed. The inner electrode is masked with a thin solution of black picein wax in trichloroethylene. A convenient technique for applying the wax is to poke a cotton swab through the hole and then apply some wax to this swab with another. Then draw the first cotton swab back out through the hole while rotating slowly. This will prevent wax from coating the junction fact to be etched. The wax should be allowed to dry for about 40 minutes. Dry nitrogen played on the area will accelerate drying. Dissolve the nickel in 40% (dilute) nitric acid. This nickel plating and stripping from the junction surface is an especially effective way to clean the junction face prior to drifting mainly due to the strongly alkaline plating solution.

Remove the adhesive tape by pulling in a direction 180° to the surface so that excessively large stress is not placed on the nickel plate. The picein wax can be removed by washing in several quantities of trico.

3. Wash crystal in methyl and dry.

4. Wrap the outside surface with indium foil and mount in the drifting apparatus as described above.

5. Fill with Freon TF and seal.

6. Apply bias very slowly (cover 30 minutes). Sudden application of bias very likely will cause breakdown. In one case, the sudden internal heating caused stress which cracked the crystal.

7. After thermal equilibrium has been reached, reset the power input to the least of 120 V max, or 500 ma max or 30 watts max, by setting the voltage and current limiters of a constant current supply. Since the power will be dissipated in a very thin surface at the junction at the onset of drifting, it is unwise to begin with high power input for the first several hours.

g. Characteristics of the Drift

If the initial power input is low enough that there is not a marked temperature rise with increased power input, i.e., the thermal impedance to the ambient is low, then one can observe the impedance increase with increasing drift depth as an increase in drift bias (at constant current). This phenomenon is indicated by the plot of bias voltage vs. time in Figure 15. The power input will eventually approach a maximum commensurate with the thermal impedance to the heat sink, and the effective electrical resistance will rise or fall after the initial drift period depending on the carrier increase with temperature (dependent on sample of germanium) which is a function of drift depth. The voltage increase with time has been similar to the curve shown in Figure 15 for every detector made, whether in gaseous or liquid ambient. The data shown is taken with a planar crystal (S#5B; current 19.4 $\pm$ 0.2 ma, T = 18 $\pm$ 2°C, 25 ohm-cm) in a nitrogen atmosphere.

The volt-current characteristic of an annulus taken 1 hour after the beginning of drift is shown in Figure 16. As the drift progresses, the reverse bias part of the curve will rise more quickly to a plateau, and rise slowly thereafter to a voltage that should exceed 120 volts without breakdown at 47°C.

After two or three hundred hours of drifting, the lithium will have migrated to all impurity and dislocation sites and become immobile since its electrostatic interaction with the applied field is reduced to nearly zero. Also, as has been mentioned above, the mobility is greater in the region of dislocations. The crystal boundary presents a complete surface of dislocations, in effect, because of the abrupt discontinuation of the diamond lattice. This will induce the lithium to migrate to the outer surface and nucleate. (If the surface were in an oxygen-bearing atmosphere the lithium would oxidize
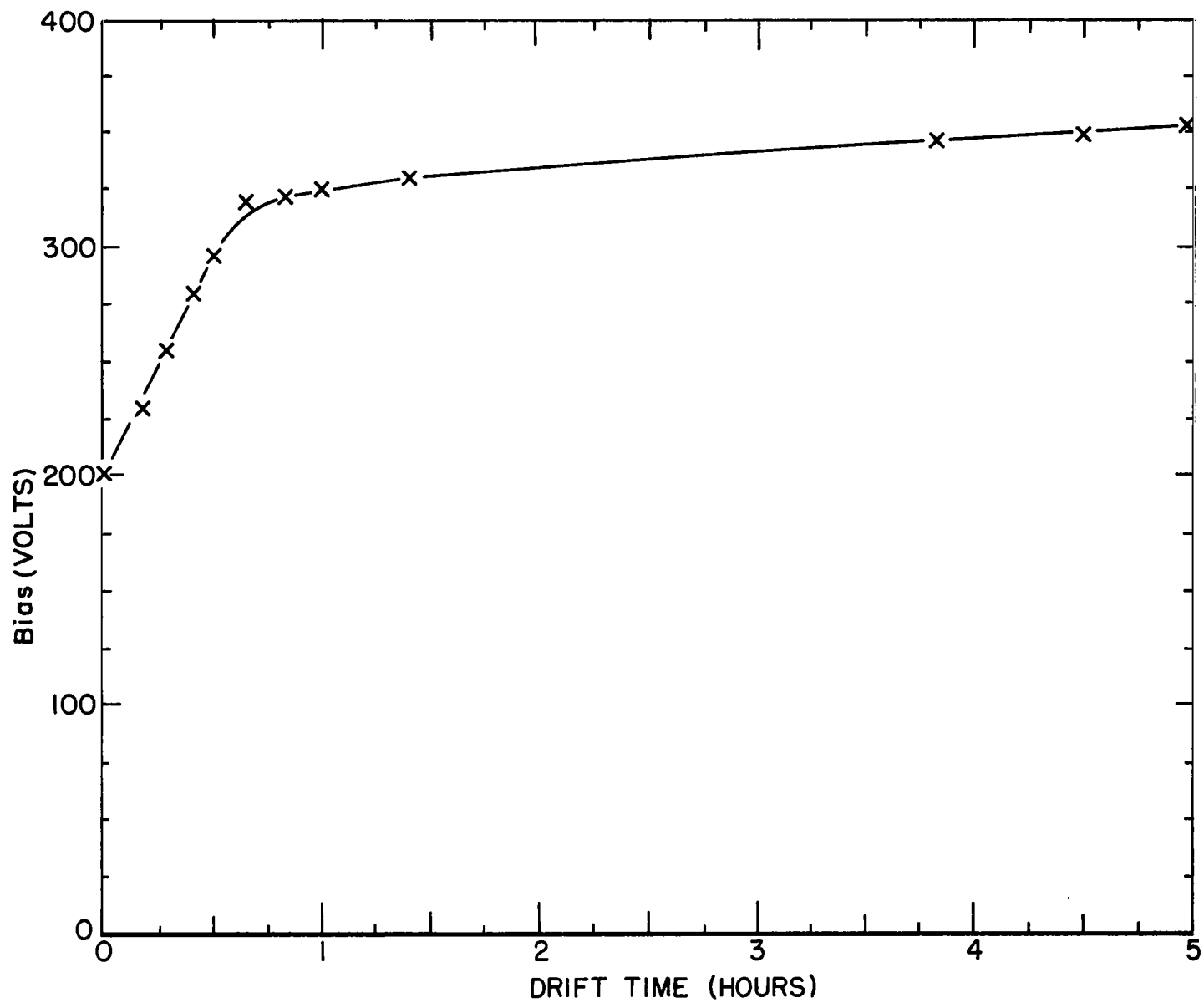
Figure 15. Bias voltage at constant current vs. time at the beginning of the drift.
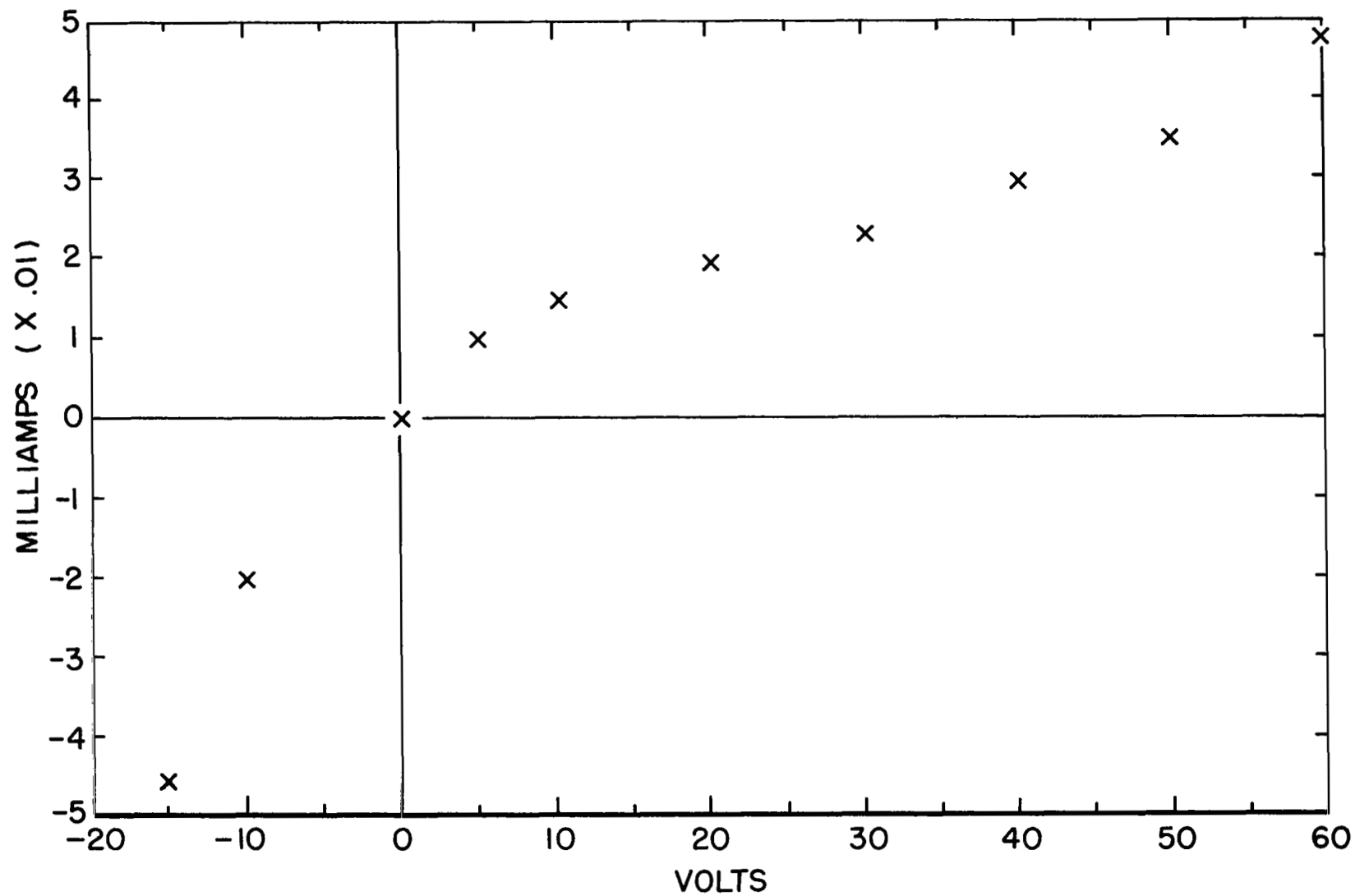
Figure 16. Diode characteristics of Ge(Li) annulus #4 at 1 hour after initiation of drift.

44

and be lost). Also, the lithium at the n-type contact will creep down this surface, reducing the electrode separation, in effect, increasing the electric field at the surface, causing the observed current to be due to surface current. Since the total drift depth is related directly to the dissipated power in the bulk material, the drift rate as predicted from the volt-amp product (calculated from the observed current) will be totally unrelated to this quantity.

It becomes necessary, when this happens, to remove the crystal from the drifting apparatus and to etch the surface of the crystal, being careful to mask the inner and outer nickel electrodes. Indications that this has become a necessary step are that the drift rate is proceeding slower than is theoretically predicted or a definite change in I-V characteristic. The drift rate can be measured by copper staining, as described in the following paragraphs.

h. Determination of Drift Depth Via Copper Staining

At any time during the drift, it is possible (and advisable every 150 hours or so) to measure the drift depth. It is also desirable to do so without the extreme temperature change that is involved in making capacitance measurements, since the recycling has been found to be deleterious to final characteristics*. The method of depth measurement by copper staining is easily performed and has the added benefit that it cleans the surface. The procedure is as follows:

1. A solution of copper sulfate is prepared.

400 ml water

24 gms copper sulfate

---

*C. Chasman, Private Communication, December 16, 1965.

2. The solution is cooled to ice temperature. This will produce good definition of the junction demarcation, since the thermally generated carriers will be reduced.

3. A copper foil is taped to the outer electrode with the same solvent-resistant tape as is used for masking. Contact is made to the inner electrode, being careful not to scratch the nickel plating.

4. Connect the lithium-rich (outer) contact to a positive voltage source, and ground the inner electrode. Pass approximately 50-75 ma through the crystal.

The crystal is now reverse biased, with the depleted region being slightly positive and the p-type germanium being biased negatively. The greatest field strength will be at the i-p interface as a consequence of reverse current compensation. The copper ions, being positively charged will plate out onto the i-p interface on the p-side. The progress of the drifting of Ge(Li) Annulus #4 can be observed in Figure 17. The conclusions drawn from this data are presented at the end of this section.

If the copper does not plate readily, after 10-15 seconds, there may be foreign matter coating the surface. There will always be a tendency for matter suspended in the freon to be attracted to and plate out on the high electric field region. This is often removed by rubbing with a cotton swab with the crystal immersed in various solvents (not acids).

5. Remove all electrodes and tape, wash in water, dip in alcohol and dry.

6. Mask as described for a routine etch with picein wax on the inside and tape on the outside.

7. Dip the crystal in 40% nitric acid until the copper disappears. Dilute and decant, etc.

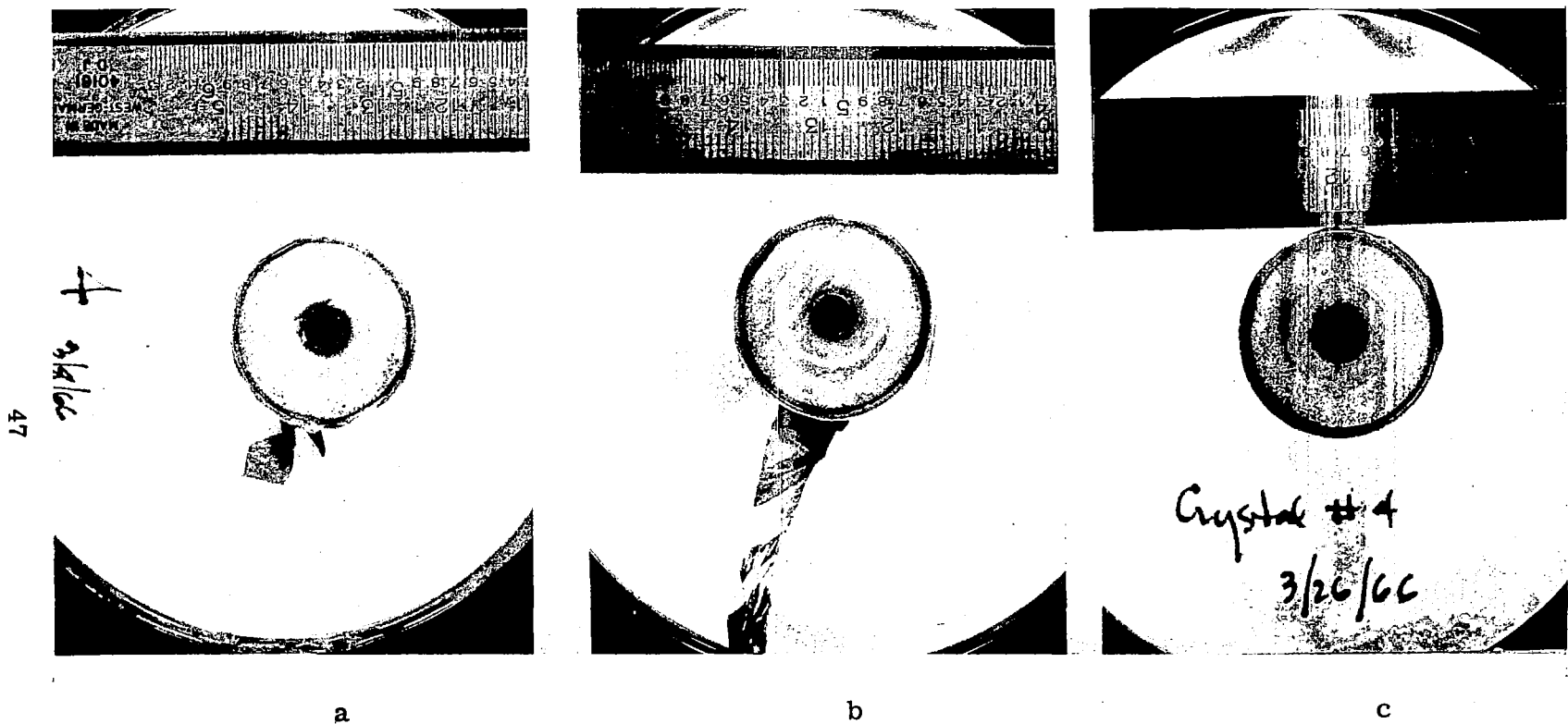8. Etch in CP4, dilute and decant, etc.

46

Figure 17. Photographs of the Ge(Li) annulus #4 junction, copper stained, at three occasions during the drift.

9. Dry and remount in the drifting apparatus.

i. The Post Drift

Because the current-induced overcompensation is an un-
avoidable by-product of rapid, high power drifting, a post drift, or "clean-up
drift" has been used as the last stage before testing. This is most effectively
done in the present apparatus, by tapering off the current during the last few
days and immersing the freon bath in ice for the last two days, or until the
voltage at a few milliamps ceases to rise. Alternatively, this can be done
in the final operating cryostat. The crystal should not be sustained in this
condition much longer than necessary to flatten the lithium distribution.
The mobility is not high enough to cause appreciable controlled drifting to
take place, but the lithium still tends to migrate over the surface of the
junction. After 10 hours of low temperature drifting, the diode characteris-
tics of Ge(Li) annulus #4 appeared as in Figure 18. After an additional 78
hours of post drift at 0°C the leakage current at 120 volts had decreased 6%
as shown. Further drifting at that temperature produced no noticeable change.
The diode was packaged after 120 hours of post-drift. No V-I curves were
measured at LN temperature for this sample as low temperature cycling was
deliberately avoided. The effect of the post-drift, as performed in this pro-
cedure are well established in the literature as a means of improving detector
characteristics[42, 43].

j. The Cryostat

The cryostat in which the detectors are mounted and used
satisfy the following criteria:[44]

1. They are vacuum tight and pass stringent leak tests.

2. They allow for continuous cooling of the detector at 77°K.

3. They are compact so that the closest possible approach to the detector
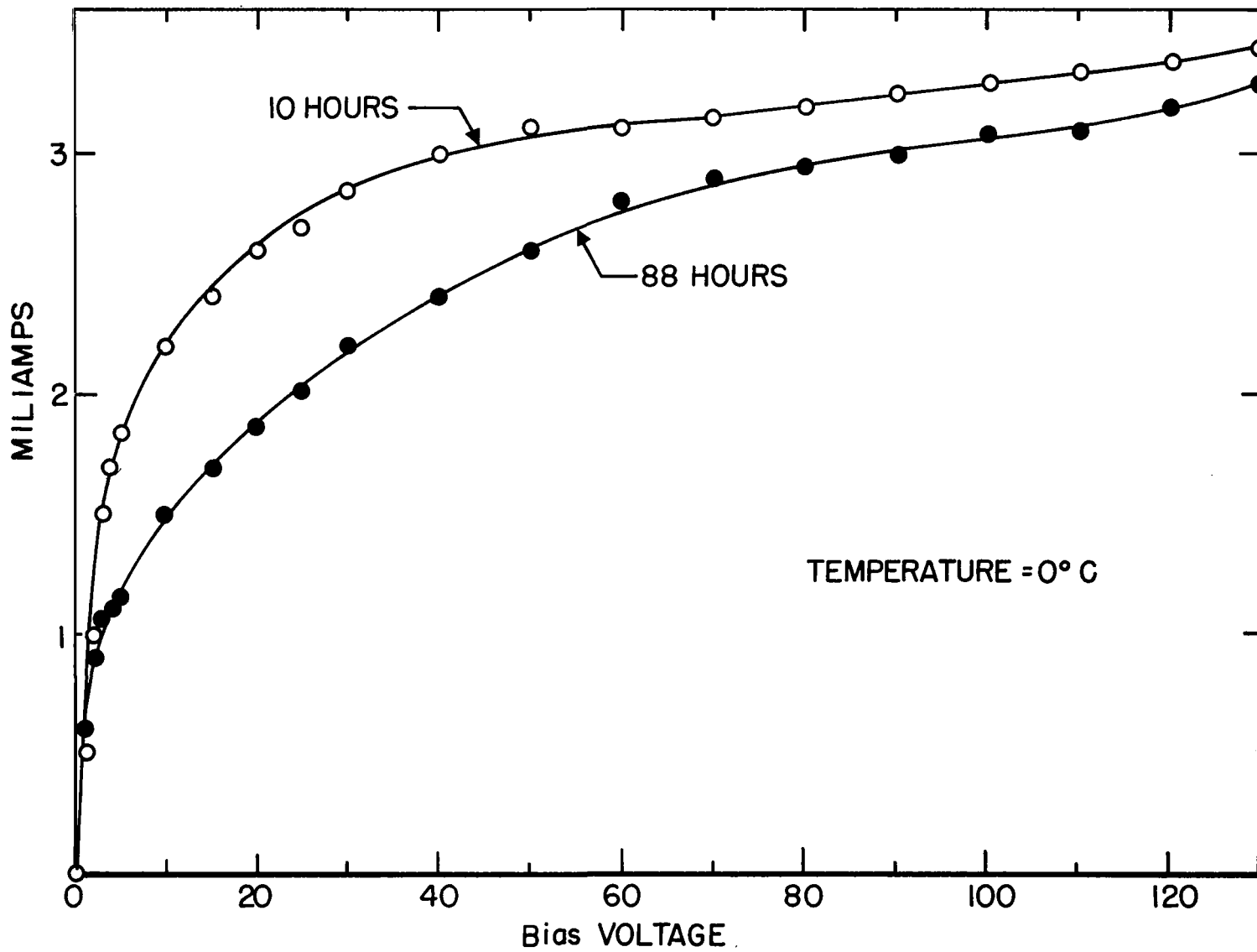is realized.

Figure 18. Diode characteristics of Ge(Li) annulus #4 during the post-drift.

4. Heat transfer is made minimal so that the refrigerant is slowly dissipated, and so the detector surface is not warmed via radiation from the cryostat walls.

The detector mounting and cryostat shown in Figure 19 is typical of that used to mount the annuli fabricated in this laboratory.

The heat absorption via radiation of a germanium surface at 77°K from a room temperature blackbody is approximately 25 mw/sq.cm. (the emissivity of germanium is 0.5). This knowledge along with the need to have a sturdy, but flexible, mounting has led to the design shown. A variety of different designs have been used for special applications. The crystal is wrapped with a fresh, cleaned layer of indium foil, set in the (gold plated) copper cradle as shown. A gold-plated copper sheet is fastened over the outside of the crystal, and a set screw is tightened so that it is secure. The copper sheet is springy enough so that deviations from being circular, coupled with the soft indium are adequate to allow for expansion on cooling[45]. The copper cradle is soldered to a copper rod that passes out of the vacuum in a variety of ways depending on the individual cryostat design. As a safety precaution against condensible vapors entering the chamber through the pumping port, a flat was soldered to the support post covering the hole. In operation the post and flap are at liquid nitrogen temperature and the flap serves as a coldtrap.

The center contact, to be connected to a negative bias, for this mounting geometry (with the outside obviously grounded) is made with a gold leaf spring contact in the same manner that the inner contact was made during drift. The contact is made dry, but a small bead of indium is melted to the gold where it will contact to avoid scratching the Ni plate. The use of gallium-indium eutectic as a wetting agent has been used on occasion, but it has been pointed out that the majority of experimentors fabricating Ge(Li)

50

Figure 19. Ge(Li) annulus mounted in a typical
cryostat.

detectors avoid it[*].

The gallium may alloy with the germanium, possibly causing strains in the material. Measurements in this laboratory have shown that the Ga-In eutectic behaves p-type on the germanium surface and this alone has discouraged its use to form the n-contact. It has been observed to spread over the applied surface quite readily, and it is not known whether it will creep over onto the delicate junction surface. Again, this uncertainty has been enough to discourage its use until further measurements have been made.

The cryostat is thoroughly cleaned, and outgased under vacuum. Its cleanliness is best gauged from the current reading on a Vacion pump. Cleaning and outgasing should be continued (after leaks are eliminated) until the current has dropped to 5 microamps[**].

The last treatment given the crystal before sealing in the cryostat is several etches with CP4, (masked) with a thorough rinsing in water afterwards. A quick dip in boiling methyl assures a clean dry surface. There are a myriad of surface treatments that have been published which are now for the most part regarded as useless; for example, dipping in hydrogen peroxide.

The cryostat has been constructed and used so that the signal lead was as short and as distant from ground surfaces as possible, to avoid excessive capacitance. This has the effect of minimizing the preamplifier noise.

4. Comparison of Radial Drifting vs. Planar Drifting

Data taken during the drifting of Ge(Li) annulus #4 (Figure 20) shows that the growth of the depletion region vs. time is somewhat more rapid

---

[*] C. Chasman, Private Communication.
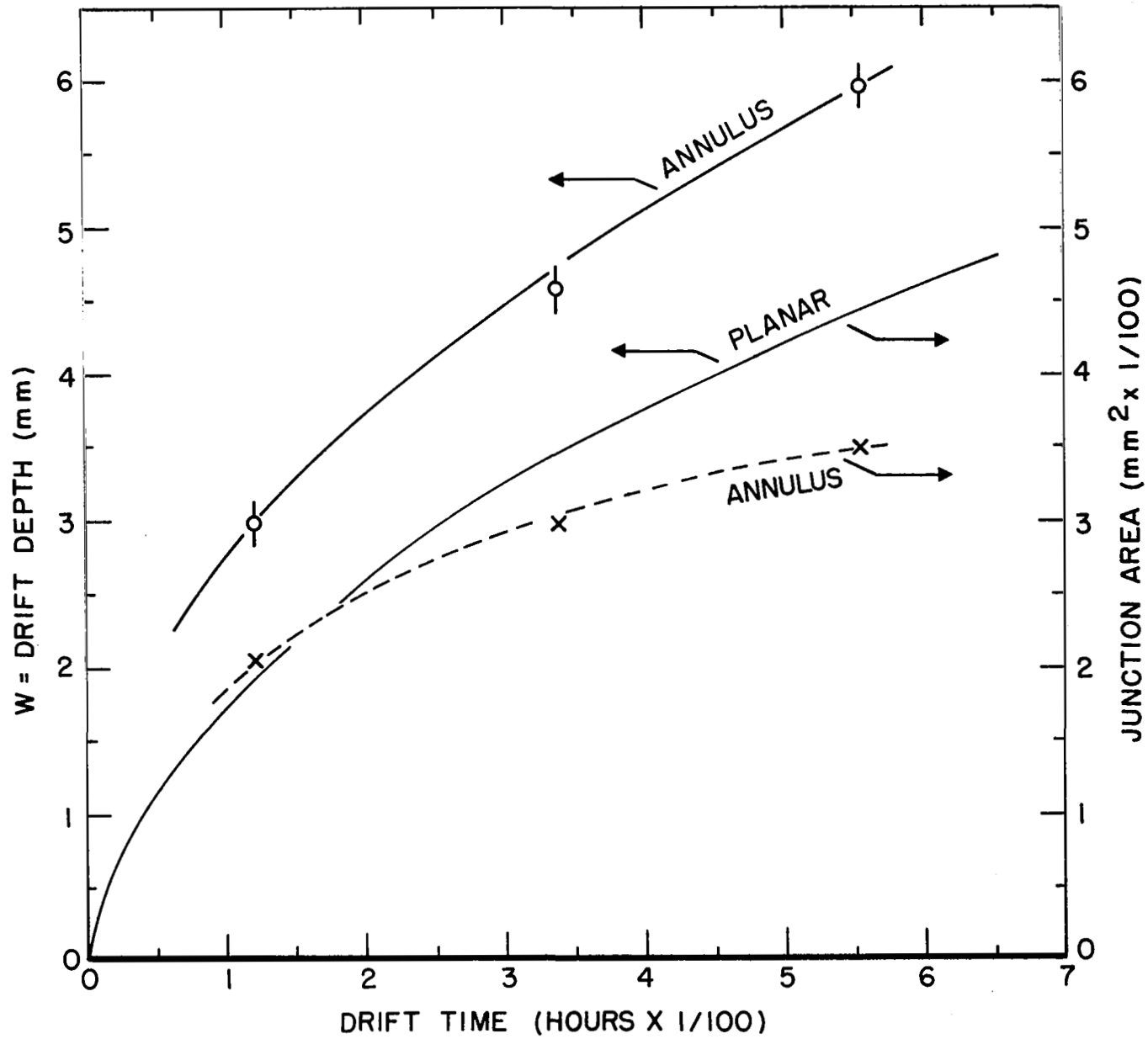
[**] H. Mann, Private Communication.

Figure 20. Junction edge area and drift depth vs. drift time. Data taken with Ge(Li) annulus #4. Planar data is theoretical.

than the planar case. The drift depth and area of the junction edge (which is directly proportional to the volume) for the annulus is plotted vs. drift time. This is to be compared with the drift depth of a planar diode, given by

$$w = \sqrt{2\mu Vt/kT}$$

and the area of a 10 mm wide planar junction plotted vs. time; the same curve applies to both parameters for the planar case, where

w is the drift depth in mm

μ is the lithium mobility at the temperature, T

V is the bias voltage

t is the drift time

The annulus was drifted at 47°C, with an average voltage of 100 volts. The outer radius is equal to 12.4 mm; the product $2\mu V$ is equal to 1.5×10^{-7}. The comparison of the two volumes (i.e., areas) is academic as the planar case is calculated for a unit cross section area, but the rate of change of area, i.e., the slope of the curves indicates that the two are nearly identical at the first stages, which is to be expected since the field in the radial geometry is nearly linear at 12 mm radius. At deeper drift depths, the radial drift rate is greater than the planar case (a natural consequence of the $1/r$ field dependence), but the rate of volume increase has become less. This is due to the compensating r^{-2} dependence of the volume in the annulus. It is hardly necessary to note that this is not particularly a shortcoming of the annular drift because the length of the cylinder is much more easily extended than the electrode area of a flat detector.

D. Operation and Testing of the Detector

   1. Capacitance Measurements

54

The initial tests made on a Ge(Li) detector are intended to determine the optimum operating conditions. It is also valuable to know the capacitance of the detector so that if noise measurements are to be made an equivalent capacitor can be substituted that is as close to the detector capacitance as possible. Confidence in the drift geometry is further reenforced if the calculated capacitance is in agreement with that measured. With the annular geometry, the capacitance is given by the equation,

$$C = 8.76/\ln(12.4/r) \text{ picofarads/cm}$$

where r is in mm. C is the capacitance of 1 cm long crystal.

The capacitance was measured by the following circuit and the subsequent calculations;
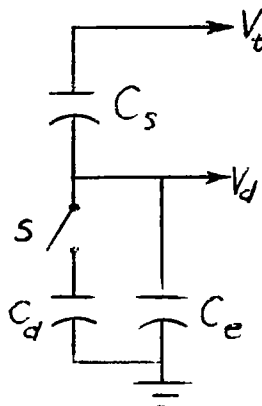
C_s = standard capac.

C_d = detector

C_e = everything else

with S closed:

$$C_s V_s = (C_d + C_e) V_d$$

$$C_d = \frac{C_s V_s}{V_d} - C_e$$

With S open:

$$C_s V_s' = C_e V_d'$$

$$C_e = \frac{C_s V_s'}{V_d'}$$

$$C_d = C_s \left(\frac{V_s}{V_d} - \frac{V_s'}{V_d'} \right)$$

The circuit was used with a pulsed voltage source as V_t (square wave generator) and the voltage V_d was measured with a voltage-sensitive amplifier (oscilloscope). The circuit used has as the standard a 100 pf capacitor and provision for applying bias to the detector during the measurements. The capacitance of Ge(Li) annulus #2 as measured this way was 59.5 pf, (using a 200 kc, 25 us wide square pulse). This gives a calculated depth of 3.7 mm $\pm$ .2 mm. The error is due to the tolerance on the standard capacitor. This depth agrees well with the depth as determined by copper staining as shown in Figure 21. This crystal was sectioned to show the uniformity of the drifted region, after being partially drifted. For bias voltage above 10 volts (to 550 volts) the capacitance did not change measurably. This attests to the fact that the depletion region is intrinsic and a very small bias is all that is needed to sweep out the diffused carriers.

2. Bias Dependent Characteristics

Figure 22 shows the typical dependence of leakage current, resolution, and pulse height (for the 662 kev Cs^{137} peak) as a function of applied bias voltage. It is significant that the pulse height reaches a constant value above 300 volts. This means that above this value the mobility of the carriers is such that the drift length is greater than the radial depletion width. If the detector were operated below this value, the peaks observed would be asymmetric, with a low energy tail caused by those carriers that were trapped and recombined before collection. The fact that all the peaks observed with this detector are symmetric normal distributions supports this data and assures that trapping is no problem. The leakage current is monotonic increasing with bias as one would suspect, but it is higher than is considered optimum (less than 10 nA). It is believed that the large leakage current on this detector is due to condensables that were trapped on the cold junction
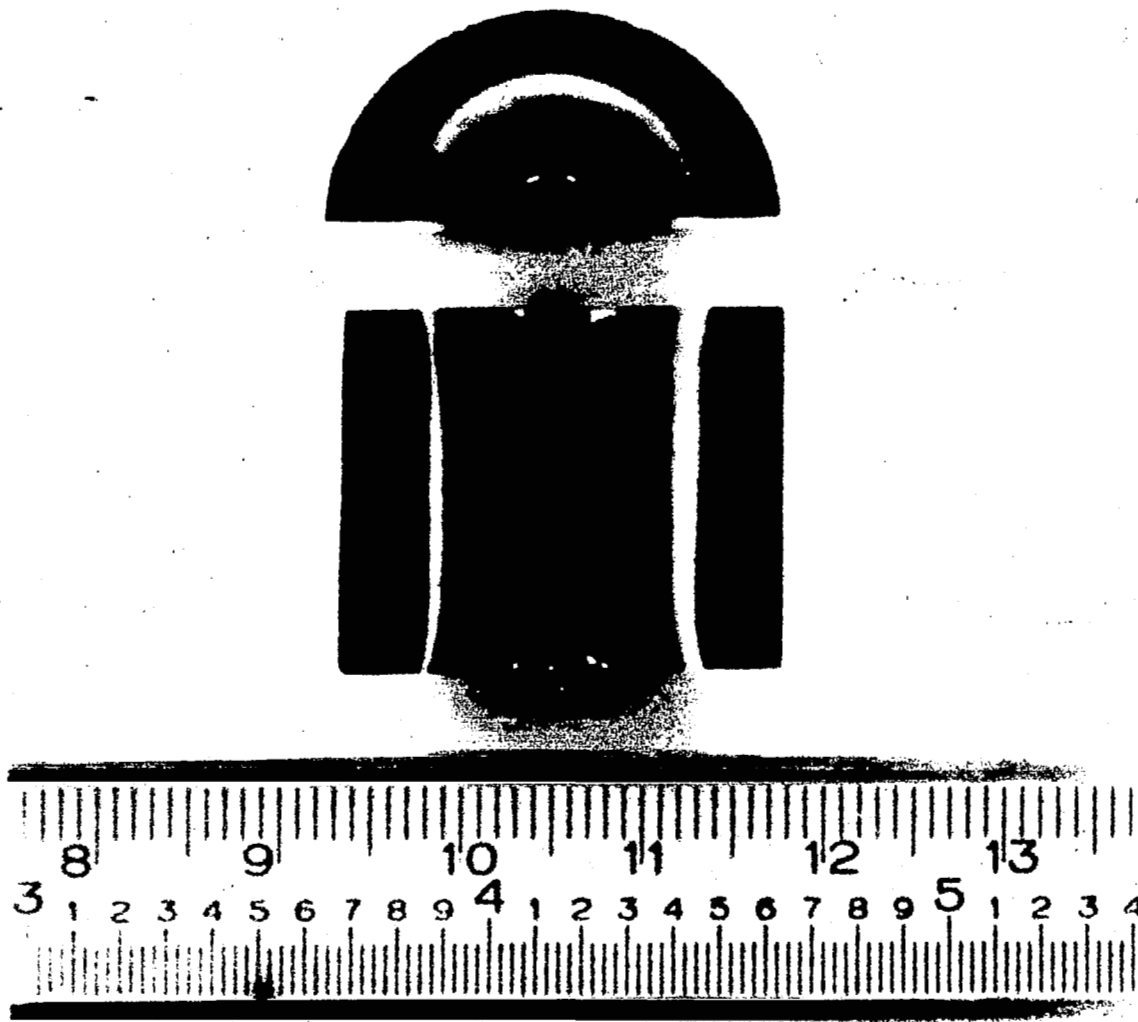
Figure 21. Ge(Li) annulus #2 cut in half and copper stained. The profile of the junction is exposed.
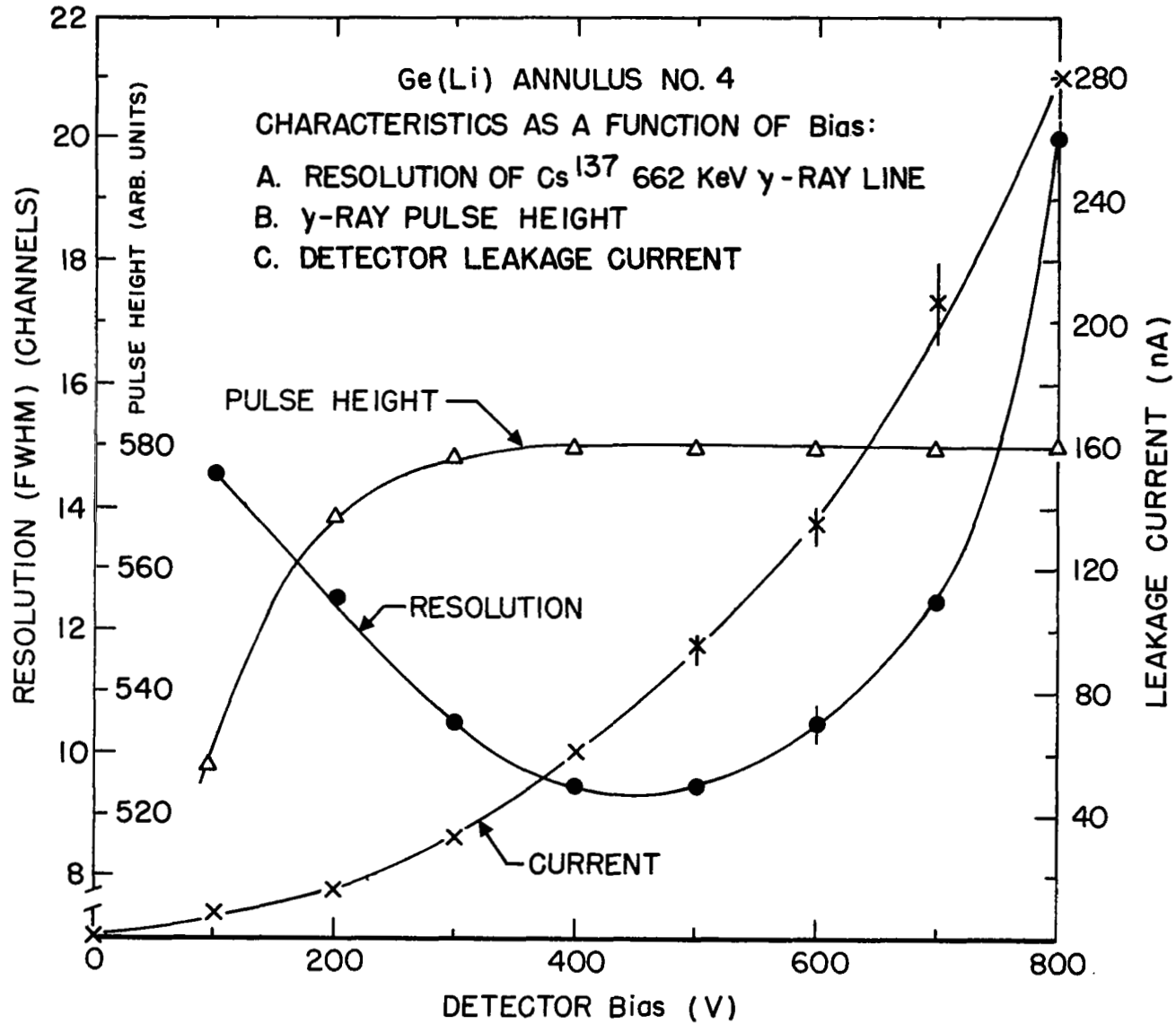
Figure 22. Detector characteristics as a function of bias voltage.

surface eminating from the cryostat walls. The measured leakage two hours
after initially cooling the detector was 7 nA, and it rose steadily for the
next 12 hours to the present value. It has changed very little in the 4
months it has been observed.

The resolution has the characteristic variation with voltage, an initial
decrease while the charge collection properties improve, followed by a gradual
deterioration caused by the increasing leakage current. The detector is being
operated at the highest possible bias commensurate with the minimum of the
resolution curve. This is to obtain maximum speed of charge collection. The
detector Ge(Li) annulus #4 is operated with a bias of 550 volts. The quality
of a detector in most respects can be quickly judged from the spectra of
selected radioisotopes. Figure 23 is a spectrum of Co^{57} with peaks at 122 KeV
and 136 KeV. These peaks, 14 KeV apart are completely resolved, the FWHM
being 6.2 KeV. The contribution of the detector itself to the FWHM is approxi-
mately 4 KeV. The low-energy noise becomes excessive below 25 KeV, for this
detector. Figure 24 is the plotted spectrum of Co^{60}. The FWHM for this spec-
trum is 7.4 for both peaks.

E. Discussion

The annular geometry makes possible the standardization of detectors for
gamma ray spectrometry for the following reasons:

1. The geometry is highly regular; i.e. the hollow core assures that the
intrinsic region remains cylindrical except for small edge effects. Therefore,
capacitance measurements and copper staining give easily interpreted informa-
tion. The uniformity of the drifting was observed by cutting in half a diode
that had been partially drifted. The result of sectioning and copper staining
is shown in Figure 25. The drift depth measured over 95% of the length was
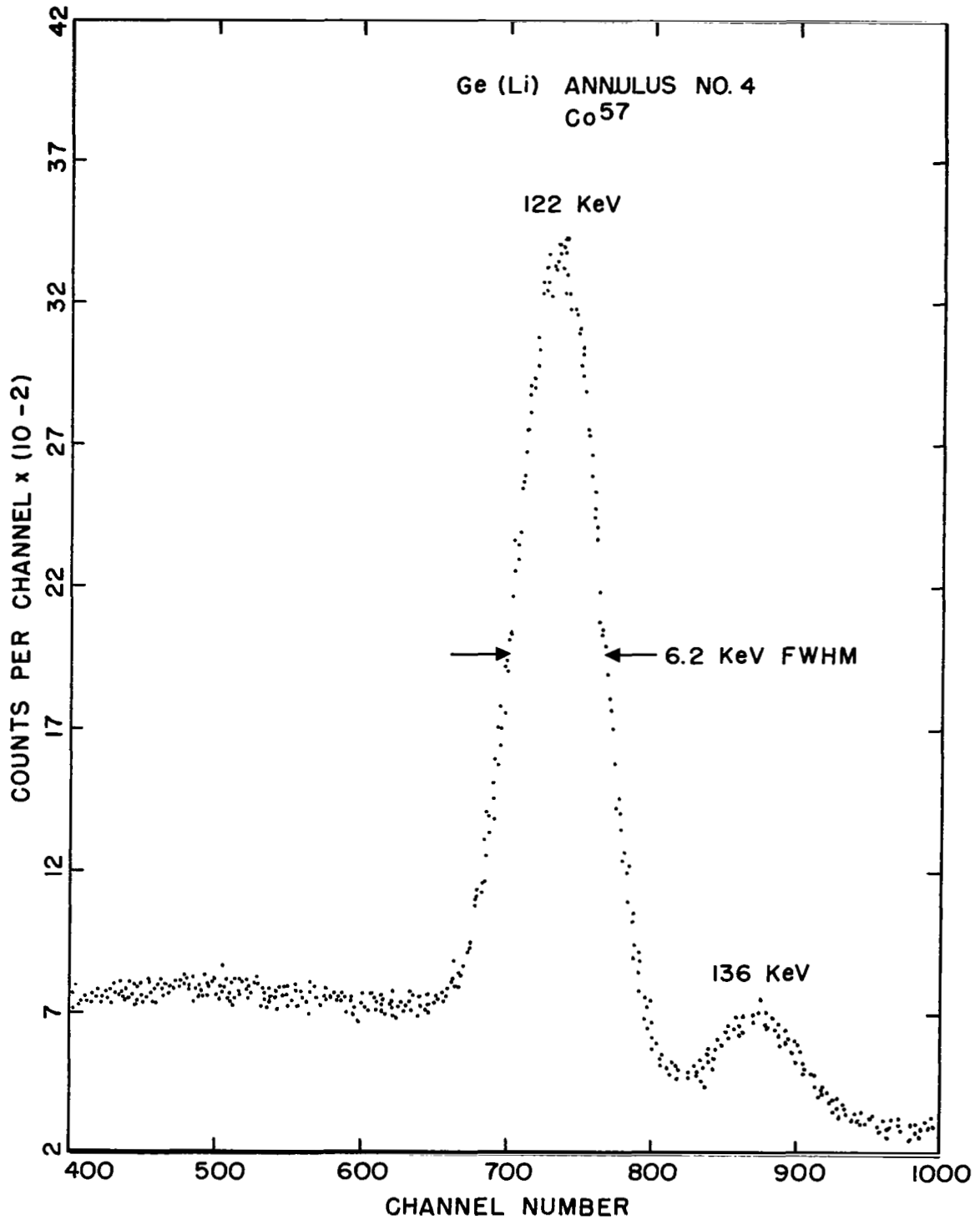found to be (4.0 ± 0.2) mm. Capacitance measurements had indicated a radial

Figure 23. Energy resolution of annulus #4 with room temperature F.E.T. preamplifier and 0.8 μ sec time constants.
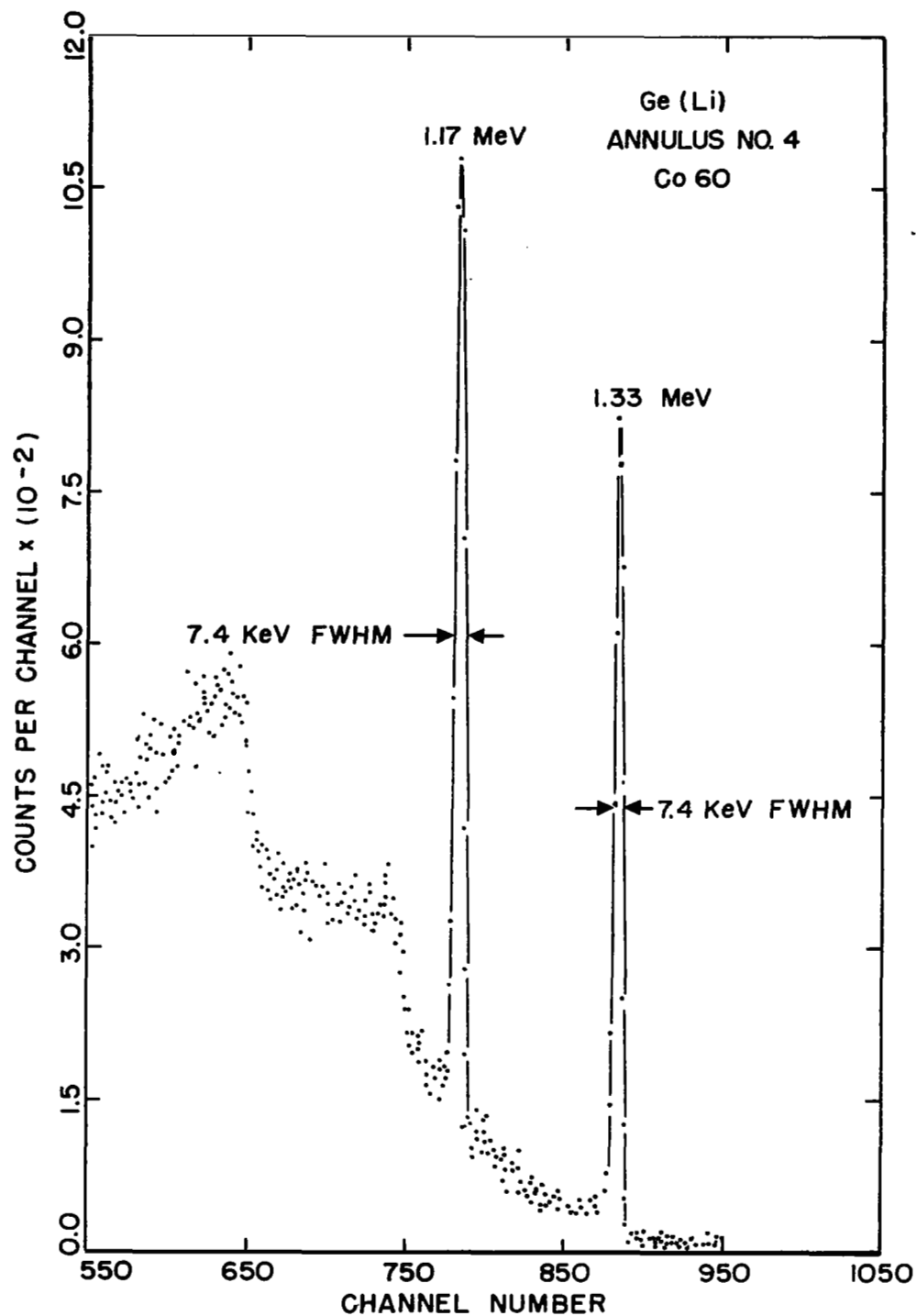
Figure 24. Energy resolution of annulus #4 with vacuum tube preamplifier and 0.8 μ sec time constants, double differentiation.
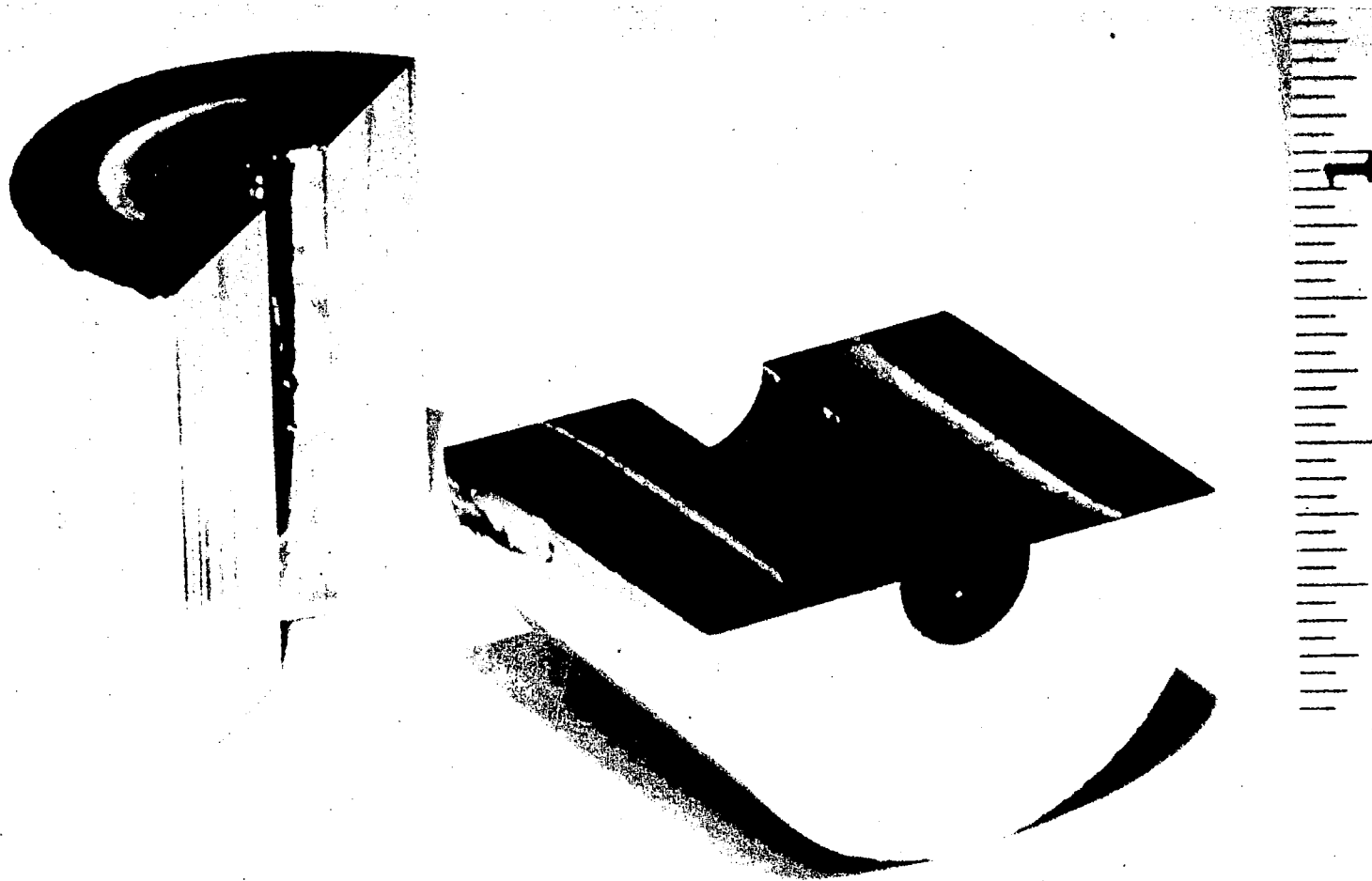
61

Figure 25. A Ge(Li) annulus is cut in half and copper stained to show the uniformity of the drifted region.

depth of 3.7 mm $\pm$ 0.2 mm. The distortion at the edges is slight, which is clearly desirable.

2. The only parameters needed to specify the detector geometry are the inner and outer diameter as well as the length of the cylinder. One is able to compare quantities such as the intrinsic efficiency of the detector with others, thus facilitating the compilation of tables of these quantities.

3. If the gamma source is placed on the axis of the annulus, the simplicity of the geometry allows interpolation of the efficiency of annuli of various sizes.

A cylinder of 1 inch o.d. drifted to a depth of 8 mm has a volume of 10 cm^3 per inch of cylinder length. The drift time, surface leakage properties, and charge collection properties are not a function of the length of the cylinder so that long detectors of large volume can be made almost as fast and easily as small ones. The only limitation seems to be homogeneity of the germanium ingot and the usefulness of the long thin shape.

The removal of the central core and the edge portions of the trapezoidal ingot eliminates the parts of the germanium ingot with the greatest dislocation density. Furthermore, the strains in these crystals are along the direction of the axis of the annulus, concentrated at the center and the edges. Drifting in the radial geometry is thus perpendicular to these ribbons of dislocations.

We believe that drifting perpendicularly to these dislocations enhances the uniformity of the drift.

Two annular detectors produced with active volumes of 8 cm^3 have each performed well as center crystals of a three crystal pair spectrometer. For a gamma ray energy of three MeV, the pair spectrometer detects approximately one out of every 1000 photons incident on the germanium crystal. Figure 26 shows a typical double-escape spectrum resulting from the $^{23}Na+d$ reaction showing

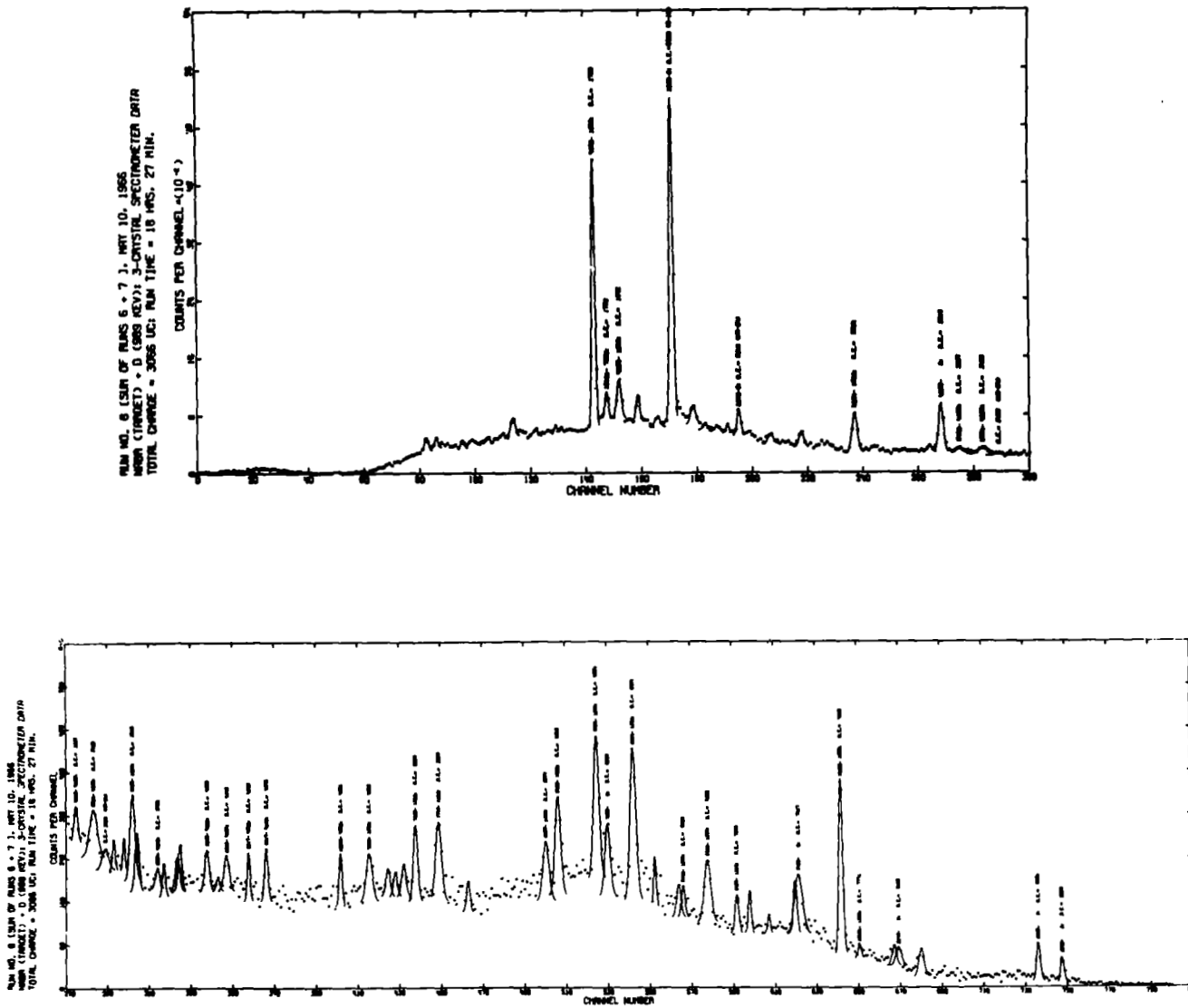Figure 26. Double-escape spectrum of ^{23}Na+d using a Ge(Li) annulus as the center crystal of a 3-crystal pair spectrometer.

transitions up to 10 MeV. The geometry used for the three crystal pair spectrometer is shown in Figure 27. The measured energy resolution for this detector was 6 keV (including electronics noise) at 122 keV. Not much effort was spent in trying to reduce leakage current as these detectors were to be used for reaction gamma rays.

The intrinsic efficiency of a 1x1 inch annular detector with a drift depth of 6 mm has been measured up to 9 MeV at several source-to-crystal distances. Standard efficiency tables and graphs similar to those available for the NaI crystal have been prepared. The sources have been placed on the axis of the annulus and the intrinsic efficiency of the detector at several distances from the source has been measured. Figure 28 shows the intrinsic efficiency as a function of incident photon energy for the photopeak, double escape peak, and single escape peak. Curves are shown for three source-to-crystal distances; 5, 10, and 20 cm.

The functional dependence on energy of the intrinsic photoefficiency, $(R_1 \epsilon_1)$, is approximated to within 3% at h = 10 cm by the equation:

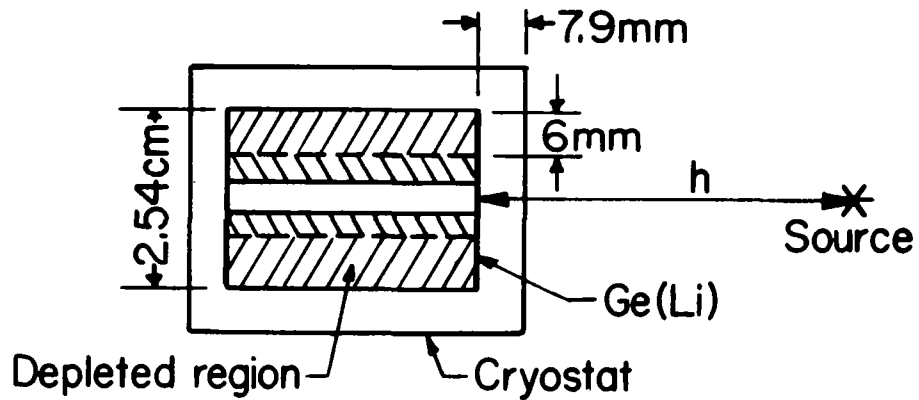$$R_1 \epsilon_1 (\%) = \exp\ (2.32 - 1.593\ E_\gamma + 0.1908 E_\gamma^2 - 0.00988 E_\gamma^3).$$

The double escape efficiency $(R_2 \epsilon_2)$ is approximated by the following equation between 2.5 MeV and 6 MeV incident photon energy to within 5%.

$$R_2 \epsilon_2 (\%) = 0.3115 + 0.3706\ E_\gamma - 0.0749\ E_\gamma^2 + 0.00412\ E_\gamma^3$$
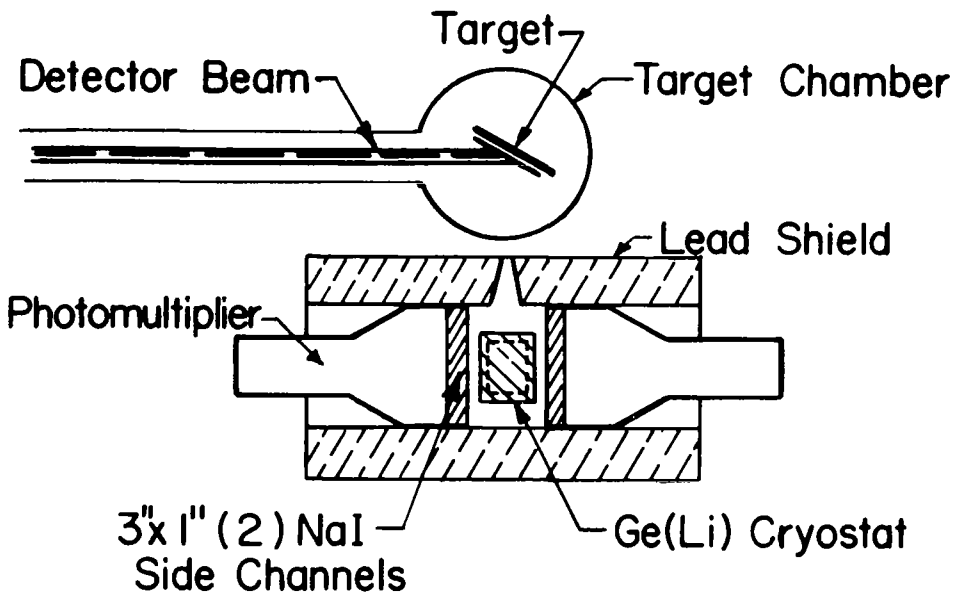
and the following equation between 6 MeV and 10 MeV,

$$R_2 \epsilon_2 (\%) = 1.1645 - 0.1304\ E_\gamma + 0.00686\ E_\gamma^2 - 0.00029 E_\gamma^3\ .$$

The photon energy, E_γ, in the above expressions is in MeV.

7.9mm

6mm

2.54cm

h

Source

Ge(Li)

Depleted region

Cryostat

Ge(Li) Annulus #4 Source-Detector Geometry

not to scale

Target

Detector Beam

Target Chamber

Lead Shield

Photomultiplier

3"x 1" (2) NaI
Side Channels

Ge(Li) Cryostat

Three-Crystal Spectrometer and Target Geometry

not to scale

Figure 27. The detector geometry for use as a spectrometer, showing
the position of the detector in the cryostat and (below) in the
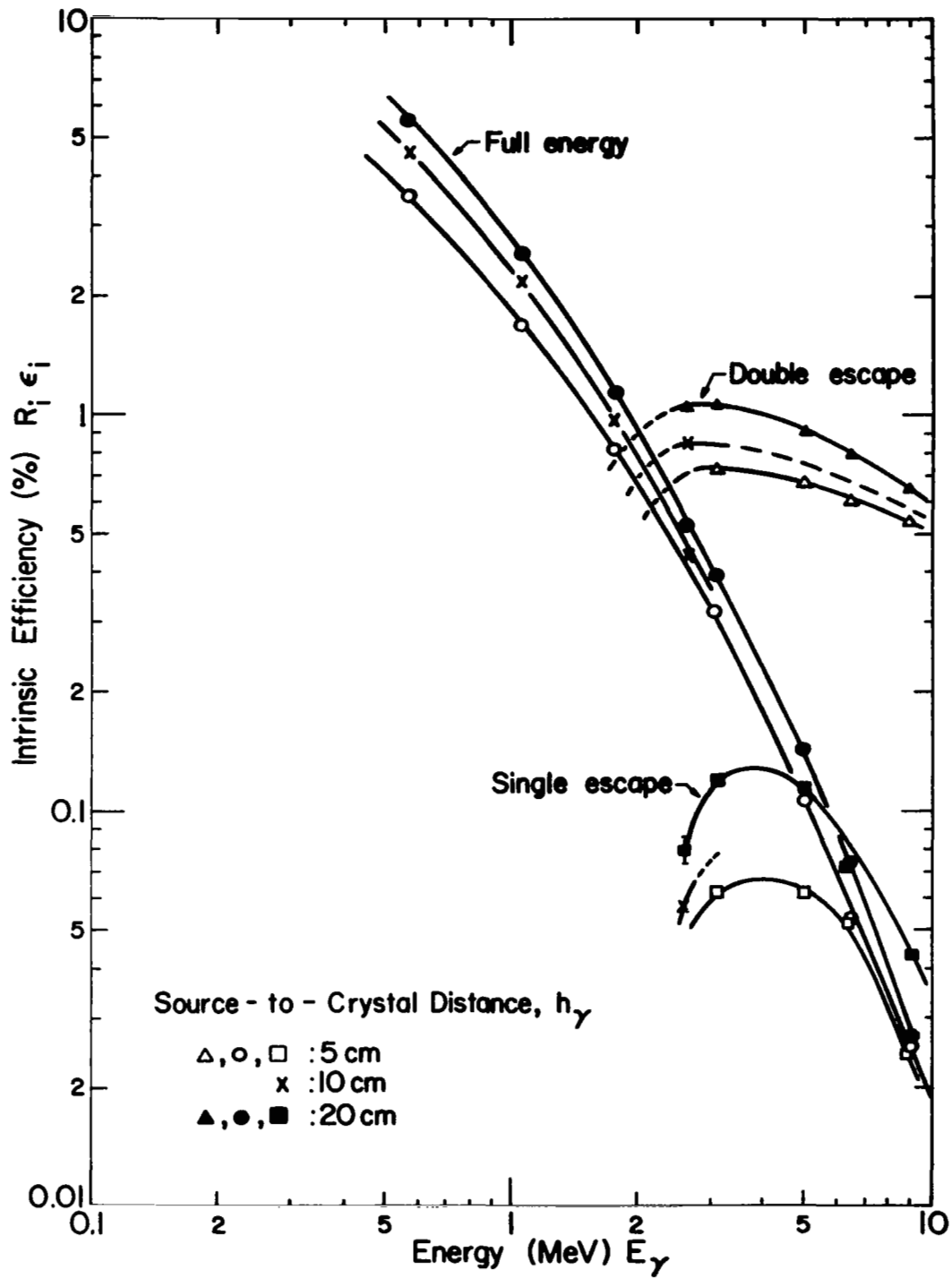three-crystal spectrometer.

Figure 28. Intrinsic efficiency of Ge(Li) annulus #4 for full-energy, double-escape and single-escape peaks.

Figure 29 shows the variation of the full-energy peak intrinsic efficiency with source-to-crystal distance for the three ^{207}Bi energies.

The relative efficiency of the 3-crystal spectrometer is shown in Figure 30. The 8 cm^3 Ge(Li) detector was mounted horizontally in a rectangular cryostat with spacing to the side crystals minimized so that the geometrical efficiency was 25%. The side channel spectra were biased at 260 keV. At 3 MeV 12% as many counts were recorded in a 3-crystal peak as would be recorded in the double-escape peak of the single crystal.

Conclusions

1. We have fabricated germanium lithium-drifted gamma detectors in the form of true coaxial cylinders. The regularity and simplicity of the geometry permitted the standardization of gamma spectroscopy techniques.

2. The techniques of spark cutting germanium have made the fabrication of the annuli feasible.

3. The annular drifted region has been shown to be uniform and depths calculated from capacitance measurements and copper staining are therefore reliable.

4. Intrinsic efficiency data for the detector used with the photons incident along the symmetry axis have been tabulated and can be used on all such detectors without ambiguity.
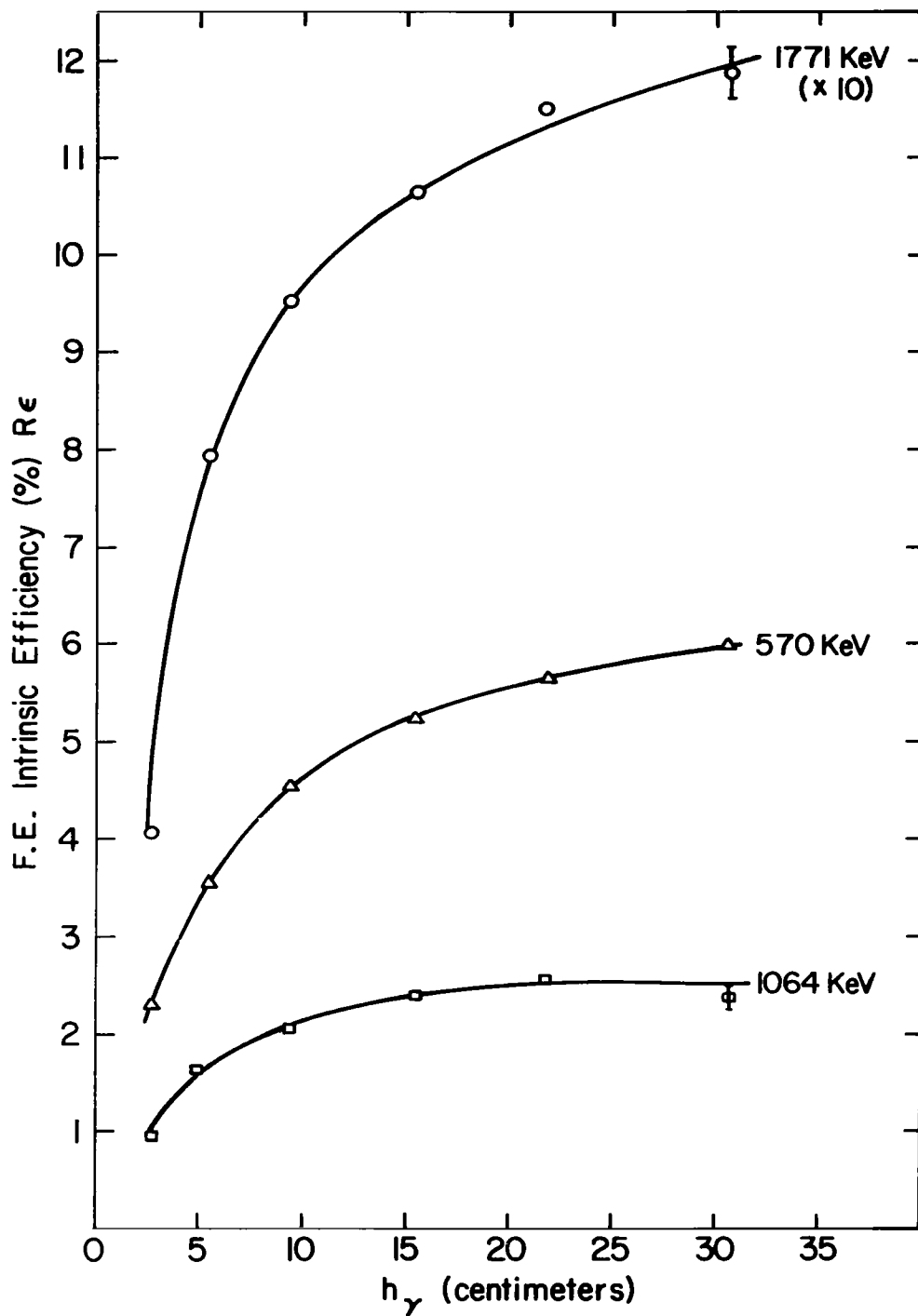
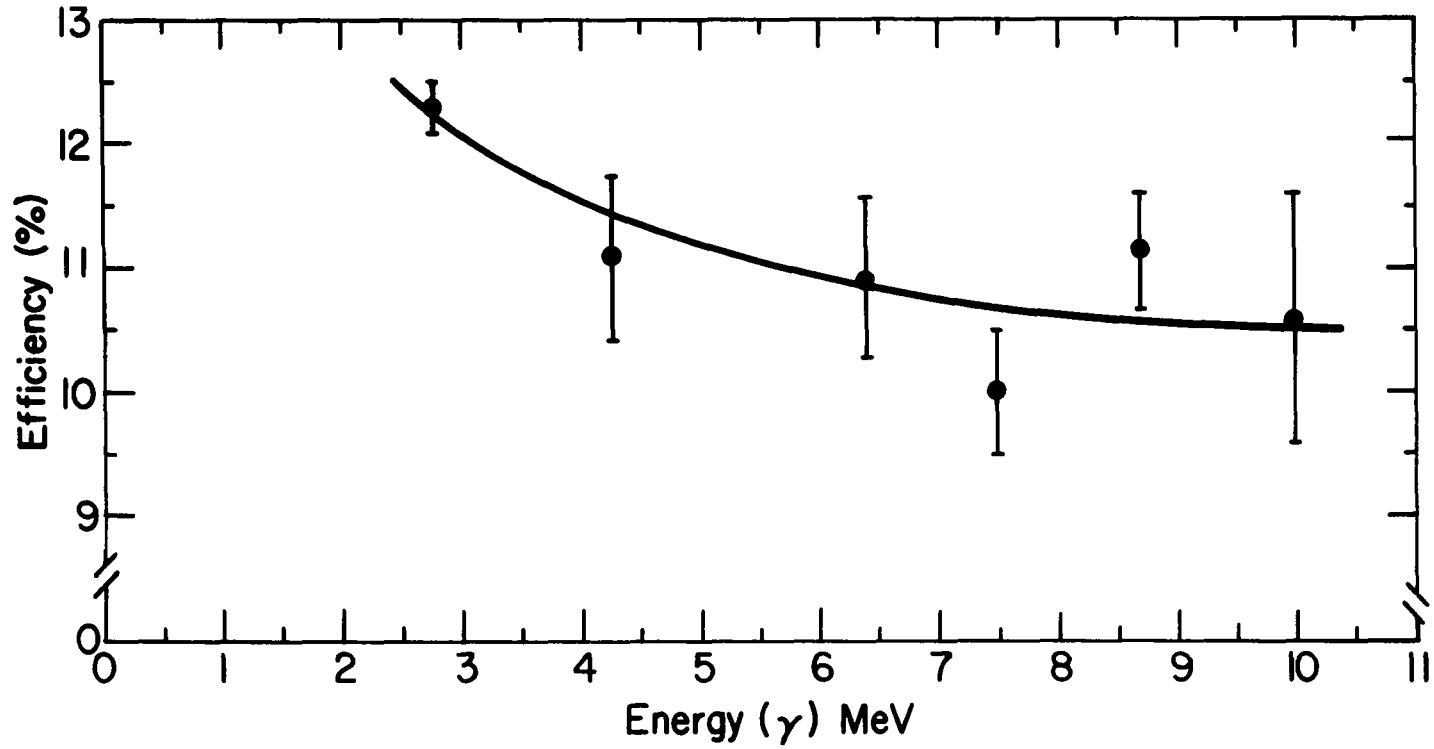Figure 29. Variation of intrinsic photoefficiency with source-to-crystal distance, h_γ.

Figure 30. The efficiency of the three-crystal spectrometer relative to the intrinsic double-escape efficiency.

APPENDIX

CHARGE DISTRIBUTION PRODUCED BY LEAKAGE CURRENT

1. Planar Case[*]

In the intrinsic zone of the n-i-p semiconductor there is a space charge being generated continuously by exciting electrons from the valence band into the conduction band. The presence of acceptor sites (from gallium doping) and donor sites (lithium ions) enhances the generation of a space charge, but in lithium drifted structure the steady state compensation is complete enough so that this is a minor contribution. The bulk-generated charge, so called because it is produced uniformly throughout the intrinsic region, is dependent on the crystal temperature.

As the drift process is carried out at elevated temperatures (47°C in this experiment) with an applied field of more than 750 V/cm, the bulk-generated space charge is observed as a current. Holes and electrons are created in equal numbers in the intrinsic zone so that the crystal remains neutral and the measured current is due to the motion of both these carriers.

In the material used for drifting, the interaction of the hole and electron currents is negligible so that the two currents can be examined separately, the total effect being due to a superposition of the two.

For the applied field E, assumed to be uniform, the velocity v of the electrons is constant. If we consider an element of volume, d, moving with the electrons, it will have also a velocity, v.

---

[*]The results of this effect for the planar case are also given in Reference (3).
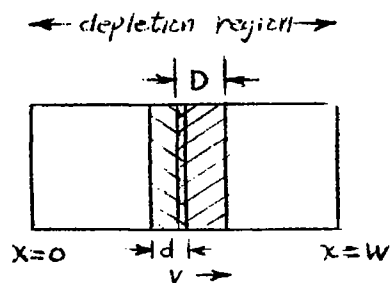
We choose as a model, a depletion region of total depth, w, divided into equal elements each element being designated as a depth D.

As the origin of the leakage current is bulk generated, each stationary element of volume, length D is a generator of charge at the rate of g/sec-cm^3.

We also construct elements of volume equal in size to D but traveling with the moving electrons (or holes, as done below), designated as "d". An element, d, passing through a fixed element, D, will have a portion of its volume which overlaps with D. During this passage, D will generate a quantity of charge and transfer it to the moving frame, d. The amount of charge produced by D and transferred to d is a function of the time of overlap and proportional to the overlap volumes as denoted as f(t).
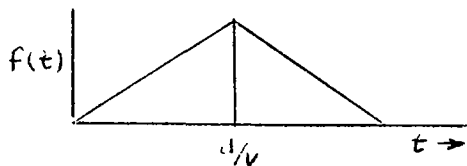
$$f(t) = \frac{v}{d}t \qquad , \quad 0 < t < \frac{d}{v}$$

$$= 2 - \frac{v}{d}t \qquad , \quad \frac{d}{v} < t < 2\frac{d}{v}$$

Total overlap of two volumes is

$$\int_0^{2d/v} f(t)\,dt = \frac{v}{d}\frac{t^2}{2}\Big|_0^{d/v} + 2t\Big|_{d/v}^{2d/v} - \frac{v}{d}\frac{t^2}{2}\Big|_{d/v}^{2d/v} = \frac{d}{v} .$$

As the rate that charge is created is g (due to electron holes), the element of length d contains $g\frac{d}{v}$ charge of either sign. If the elements are infinitesimal as well as the sources (for the elements are really their own sources) and we represent the density as N (cm^{-3}), then

$$dN = g\frac{dx'}{v}$$

The total charge in each element is the sum of all charges between x' = 0 and x' = x (v assumed constant)

$$N = \int_{0}^{x} g\,\frac{dx'}{v} = \frac{gx}{v} = \frac{gx}{u\,E} \quad ,$$

$$\text{charge density of electrons} = -\frac{e\,g\,x}{\mu_N\,E} \quad .$$

Similarly,

$$\text{charge density of holes} = +\frac{e\,g\,(w-x)}{\mu_P\,E} \quad ,$$

where μ_N and μ_P are the mobilities of electrons and holes respectively, and w is the width of the depletion zone.

For this process compensation is exact when

$$\left| \frac{-e\,g\,x}{\mu_N\,E} \right| = \left| \frac{e\,g\,(w-x)}{\mu_P\,E} \right| \quad ,$$

or, when

$$x_c = \frac{w\,\mu_N}{\mu_P + \mu_N}$$

The process is illustrated graphically below.
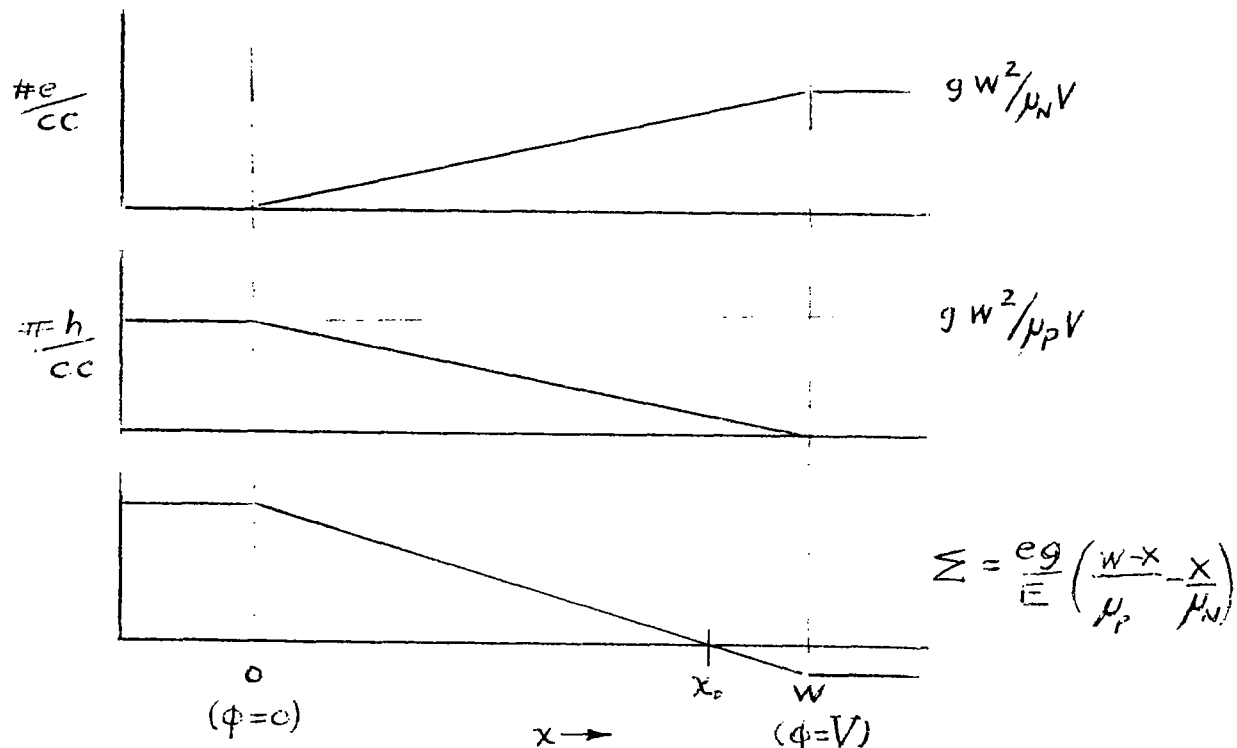
for germanium[37] @ 300°K: $\mu_N = 3800$, $\mu_P = 1800$

$$X_o \approx \frac{2 W \mu_P}{\mu_P + 2 \mu_P} = \frac{2}{3} W.$$

2. Cylindrical Radial Geometry

In order to derive the charge distribution due to a cylindrical radial collecting field, it must first be demonstrated that for a radial field with a charge injection at any radius, the charge density is constant as the charge is swept inward.

Given: Two charges at r_1 and r_2 and an element of area (volume extension is trivial) bounded by r_1 and r_2.
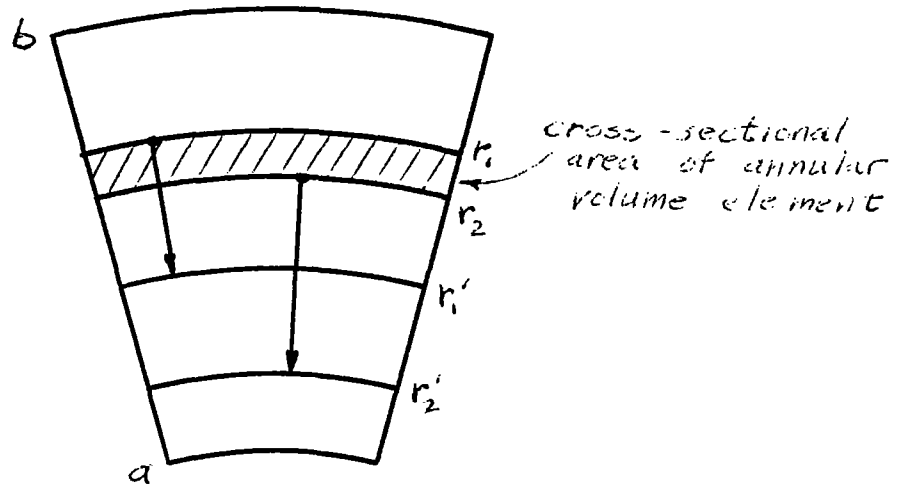

The initial charge density in the area A is exactly

$$d = \frac{2}{\pi (r_1^2 - r_2^2)} \quad .$$

We will find the density at any arbitrary time later by calculating the traversal of r_1 and r_2 to r_1' and r_2' respectively.

The potential and field are given by

$$\phi = \frac{V_c}{\ln \frac{a}{b}} \left(\ln \frac{r}{b} \right) \quad ,$$

$$E = - \frac{V_o}{\ln \frac{a}{b}} \frac{1}{r} \quad .$$

The equations for E and ∅ are zeroth order, i.e., they assume that the charge under consideration does not perturb the applied field. Under the influence of the applied field charges will move with velocity $v = \mu E$, or

$$v = -\mu \, C/r \quad ,$$

where $C = \dfrac{V_o}{\ln\frac{a}{b}}$, and μ is the mobility of the charge.

$$\frac{dr}{dt} = -\mu C/r \quad ,$$

or

$$r^2 = -2\mu Ct + C' ,$$

at $t = 0$, $r = r_1$, therefore $C' = r_1^2$,

and

$$r = \sqrt{-2\mu Ct + r_1^2} \quad .$$

i.e.

$$\frac{r_1^2 - r^2}{2\mu C} = t \; .$$

So, the distance traveled, $R_1 = r_1 - r_1'$, is

$$R_1 = -\int_{t_i}^{t} v \, dt = \int_{t_i=0}^{t} \frac{\mu C \, dt}{\sqrt{-2\mu Ct + r_1^2}}$$

$$= -\sqrt{-2\mu Ct + r_1^2} \Big|_{0}^{t}$$

$$= r_1 - \sqrt{-2\mu Ct + r_1^2}$$

Similarly,

$$R_2 = r_2 - r_2' = r_2 - \sqrt{-2\mu Ct + r_2^2} \; .$$

We can now compute the charge density at a time, t, later.

$$\text{Final Density} = \frac{2}{\pi(r_1'^2 - r_2'^2)} \; .$$

$$r_1' = r_1 - R_1 \; ,$$

$$r_1' = +\sqrt{-2\mu Ct + r_1^2} \; ,$$

and

$$r_2' = +\sqrt{-2\mu Ct + r_2^2} \; .$$

$$\text{Final Density} = \frac{2}{\pi[(-2\mu Ct + r_1^2) - (-2\mu Ct + r_2^2)]}$$

$$= \frac{2}{\pi(r_1^2 - r_2^2)} = initial \; density.$$

So, the charge density is independent of time and equal to the value given at the time of its injection into the field.

Now, we can calculate the charge density at any radius, r, in a cylindrical detector due to charge generation only. The methods used in the planar case are now applicable, since charge density has been shown to remain unaffected by radial geometry.

We assume that throughout an element of volume bounded by the domain of dr, the velocity is given by its instantaneous value proportional to $\frac{1}{r}$. To show the validity of this assumption,

$$v = \frac{\mu C}{r} \quad , \quad dv = \frac{-\mu C}{r^2} dr$$

$$\frac{dv}{v} = \frac{-\mu C}{r^2} \frac{r}{\mu C} dr = -\frac{dr}{r}$$

Since

$$dr \ll r, \quad v + dv = v - \frac{v}{r} dr \simeq v$$

So the charge density at any $\quad r = -\int_{r=b}^{r} g \frac{dr}{v}$

$$= \int_{b}^{r} -g \frac{r\,dr}{\mu C}$$
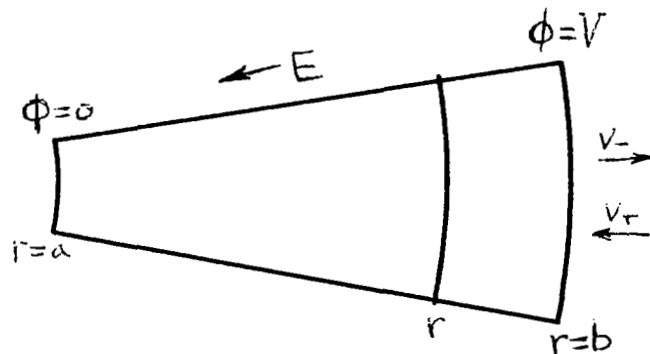
$$= \frac{-g r^2}{2 \mu C} \Big|_{b}^{r} = \frac{-g}{2\mu C}(r^2 - b^2) = \frac{g}{2\mu C}(b^2 - r^2)$$

Note that this solution holds for + or − charges since, except for sign, $v = \pm \mu C/r$ gives identical results.

However for negative charges, the total charge density at a given radius, the integration is $\quad \int_{r=a}^{r} g \frac{r\,dr}{\mu C} = \frac{g}{2\mu C}(r^2 - a^2)$

78

total charge density = (hole density + electron density) and charge is
exactly compensated when the sum is zero, i.e., when,

$$\frac{9}{2\mu_N C}\left(r_c^2 - a^2\right) = \frac{9}{2\mu_P C}\left(b^2 - r_c^2\right)$$

$$r_c^2 - a^2 = \frac{\mu_N}{\mu_P}\left(b^2 - r_c^2\right)$$

$$r_o = \sqrt{\frac{a^2\mu_P + b^2\mu_N}{\mu_N + \mu_P}}$$

For a specific case let b = 3a

$$r_o = a\sqrt{6.4} = 2.54\ a$$

REFERENCES

1. D. V. Freck and J. Wakefield, Nature **193**, 669 (1962).

2. Charles R. Gossett, <u>Nuclear Research with Low Energy Accelerators</u>, ed. J. B. Marion and D. M. Van Patter, (Academic Press, New York, 1967), p. 1.

3. J. M. Taylor, <u>Semiconductor Particle Detectors</u>, Butterworth, London (1963).

4. G. Dearnaley and D. C. Northrop, <u>Semiconductor Counters for Nuclear Radiations</u>, Wiley, New York (1963).

5. G. T.Ewan and A. J. Tavendale, <u>High-Resolution Studies of Gamma-Ray Spectra Using Lithium-Drift Germanium Gamma-Ray Spectrometers</u>, Can. J. Phys. **42**, 2286 (1964).

6. U. Fano, Ionization Yield of Radiations. II. <u>The Fluctuations of the Number of Ions</u>, Phys. Rev. **72**, 26 (1947).

7. W. van Roosbroeck, <u>Theory of the Yield and Fano Factor of Electron-Hole Pairs Generated in Semiconductors by High-Energy Particles</u>, Phys. Rev. **139** A1702 (1965).

8. S. Antman, D. Landis and Pehl, <u>Measurements of the Fano Factor and the Energy per Hole-Electron Pair in Germanium</u>, UCRL-16317 (1965).

9. H. M. Mann et al., <u>Observations on the Energy Resolution of Germanium Detectors for 0.1-10 MeV Gamma Rays</u>, Presented 10th Scint. and Semicond. Symp., Washington, D. C., March 1966.

10. H. M. Mann, <u>Limit of Energy Resolution and Fano Factor for 1-10 MeV γ-Rays in Germanium Detectors</u>, Bull. Am. Phys. Soc. **11**, 127 (1966).

11. A. J. Tavendale, <u>Semiconductor Lithium Ion Drift Diodes as High Resolution Gamma-Ray Pair Spectrometers</u>, Presented at 9th Scint. and Semicond. Symp., Washington, D. C., February 1964.

12. W. Shockley and W. T. Read, <u>Statistics of the Recombination of Holes and Electrons</u>, Phys. Rev. <u>87</u>, 835 (1952).

13. D. C.Northrop and O. Simpson, <u>Semiconductor Counters, I. Theory</u>, Proc. Phys. Soc. <u>80</u>, 262 (1962).

14. W. Shockley, Bell System Tech. J. <u>30</u>, 990 (1951).

15. B. R Nag, P. Das, H. Paria and M. H. Engineer, <u>Hot Carrier Conduction Hall Mobility and Injection Characteristics of p-Type Germanium</u>, Physica <u>31</u>, 33 (1965).

16. A. J. Tavendale and G. T. Ewan, <u>A High Resolution Lithium Drifted Germanium Gamma-Ray Spectrometer</u>, Nucl. Inst. and Meth. <u>25</u>, 185 (1963).

17. H. M. Mann, et. al., <u>Preparation of Large Volume Planar Germanium Detectors and Results of Their Use in Nuclear Physics Experiments</u>, Presented 10th Scint. and Semicond. Symp., Washington, D. C., March 1966.

18. G. L. Miller, et. al., <u>Semiconductor Particle Detectors</u>, Annual Review of Nuclear Sci. <u>12</u>, 189 (1962).

19. E. M. Pell, <u>Ion Drift in an n-p Junction</u>, J. Applied Phys. <u>31</u>, 291 (1960).

20. F. J. Morin and H. Reiss, <u>Precipitation of Lithium in Germanium</u>, J. Phys. Chem., <u>3</u>, 196 (1957).

21. J. R. Carter and R. A. Swalin, <u>On the Kinetics and Mechanism of the Precipitation of Lithium from Germanium</u>, J. Appl. Phys. <u>31</u>, 1191 (1960).

22. R. Henck, et. al., <u>Drift Rate and Precipitation of Lithium in Germanium</u>, Presented 10th Scint. and Semicond. Symp., Washington, D. C., March 1966.

23. G. A. Armantrout, <u>Ambient Storage Effects and Mounting Problems of Very Large Volume Ge LID Detectors</u>, UCRL-14263.

24. C. S. Fuller, <u>Diffusibility and Solubility of Copper in Germanium</u>, Phys. Rev. <u>93</u>, 1182 (1954).

25. J. M. Palms and A. H. Greenwood, <u>Thermoelectric Control Apparatus for the Fabrication of Thick Lithium-Drifted Germanium Detectors</u>, Rev. Sci. Insts. <u>36</u>, 1209 (1965).

26. W. C. Dunlap, <u>Diffusion of Impurities in Germanium</u>, Phys. Rev. 94, 1531 (1954).

27. J. Takacs, <u>The Depletion Depth of Lithium-Ion Drift Detectors as a Function of the Time, Voltage and the Diffusion Constant</u>, Nucl. Inst. and Meth. 33, 171 (1965).

28. F. Goulding and W. Hansen, <u>Leakage Current in Semiconductor Junction Radiation Detectors and Its Influence on Energy-Resolution Characteristics</u>, Nucl. Insts. and Meth. 12, 249 (1961).

29. A. J. Tavendale, <u>A. Germanium Lithium Drifted Diode With Guard-Ring for γ-Ray Spectroscopy</u>, Nucl. Insts. and Meth. 36, 325 (1965).

30. H. L. Malm, A. J. Tavendale and I. L. Fowler, <u>A Large-Volume, Coaxial Lithium-Drift, Germanium Gamma-Ray Spectrometer</u>, Can. J. Phys. 43, 1173 (1965).

31. H. L. Malm and I. L. Fowler, <u>Large-Volume Coaxial Germanium Gamma-Ray Spectrometers</u>, AECL 2504 (1956).

32. A. J. Tavendale, <u>A Large, Coaxial, Lithium-Drift Germanium Diode for Gamma-Ray Spectroscopy</u>, AAEC/TM299 (1965).

33. H. L. Malm, <u>Improvements in Large Volume Coaxial Germanium Spectrometers</u>, Presented at 10th Scint. and Semicond. Symp., Washington, D. C. (1966).

34. E. M. Pell, <u>Effect of Li-B Ion Pairing on Li + Ion Drift in Si</u>, J. Appl. Physics 31, 1675 (1960).

35. R. J. McIntyre, <u>Photon Detection Processes in Semiconductors</u>, RCA Victor, Ltd., Montreal, Canada, ECRDC Project T68, Report #1, (1963).

36. D. R. Turner, <u>Electroplating Metal Contacts on Germanium and Silicon</u>, J. Electrochem. Soc. 106, 786 (1959).

37. B. A. Irving, <u>The Chemical Polishing of Germanium</u>, J. Electrochem. Soc. 109, 120 (1959).

38. T. E. Burgess, <u>Chemical Etching of Germanium in $HF-HNO_3-H_2$ Solutions</u>, J. Electrochem. Soc. 104, 341 (1962).

39. B. I. Boltaks, <u>Diffusion in Semiconductors</u>, Trans. J. I. Carasso, Academic Press, New York (1963).

40. M. B. Prince, <u>Drift Mobilities in Semiconductors. I. Germanium</u>, Phys. Rev. <u>92</u>, 681 (1953).

41. M. V. Sullivan and J. H. Eigler, <u>Electroless Nickel Plating for Making Ohmic Contacts</u>, J. Electrochem. Soc. <u>104</u>, 226 (1957).

42. A. J. Tavendale, <u>Large Germanium Lithium-Drift p-i-n Diodes for Gamma-Ray Spectroscopy</u>, AECL-2196 (1965).

43. A. J. Tavendale, <u>Reduction of Carrier Trapping in Germanium Lithium-Drift γ-Ray Spectrometers</u>, Rev. Sci. Insts. <u>36</u>, 1275 (1965).

44. ·C. Chasman and R. A. Ristinen, <u>A Cryostat for Semi-Conductor Gamma-Ray Detectors</u>, BNL 8692, December 1964.

45. Goldsmith, et. al., <u>Handbook of Thermophysical Properties of Solid Materials</u>, MacMillian, Vol. I, 305-306 (1961).